Results in Engineering 27 (2025) 106880

Contents lists available at ScienceDirect

Results in Engineering

journal homepage: www.sciencedirect.com/journal/results-in-engineering

Research paper

IIPQ controlled three phase three level four wire T-type vienna rectifier for high efficient off board fast EV charging station with enhanced system stability

Suresh Kalichikadu Paramasivam [a,*], Ramesh Senniyappan [b], Senthil Kumar Ramu [c], Senthilkumar Mani [d]

[a] Department of Electrical and Electronics Engineering, Sri Krishna College of Technology (Autonomous), Coimbatore, Tamil Nadu, India
[b] Department of Electrical and Electronics Engineering, K.S.R. College of Engineering (Autonomous), Tiruchengode, Tamil Nadu, India
[c] School of Electrical Engineering, Vellore Institute of Technology, Chennai, Tamil Nadu, India
[d] Department of Electrical and Electronics Engineering, PSG Institute of Technology and Applied Research (Autonomous), Coimbatore, Tamil Nadu, India

ARTICLE INFO

Keywords:
Fast EV Charging
T-Type Vienna rectifier
Photovoltaic systems
Improved instantaneous real and reactive power control strategy
Power quality
Total harmonic distortion

ABSTRACT

Nowadays, the integration of fast Electric Vehicle (EV) charging station with microgrid becomes very challenges due to non-linear behavior of load unit. These charging unit produce harmonic distortions which reduce the power quality. To ensuring the stable voltage and current profile as per IEEE standard while connecting Grid-to-Vehicle (G2V) has becomes challenging issue. In this paper, an efficient off board 3P3L4W (Three-Phase Three-Level Four-Wire) T-Type Vienna Rectifier (TTVR) for fast EV charging stations with suppressed Total Harmonic Distortion (THD) level and power quality enhancement is presented. TTVR interfaced with Improved Instantaneous real and reactive power (IIPQ) control strategy to maintain low switching losses, enhanced steady state and dynamic load response. Hence, this proposed Fuzzy Logic Controller based IIPQ control strategy has been employed to maintain constant DC-Link voltage and capacitor voltage VC1, VC2. This method is validated by using MATLAB and experimental validation also carried with 15KW laboratory prototype using digital signal peripheral Interface controller (dsPIC30F4011), Rapid Hyper-fast Recovery Glass (RHRG30120) power diodes and Silicon Carbide Metal-Oxide-Semiconductor Field-Effect Transistors (SiC MOSFETs IRFP260) switches to maintain high switching stress and low ON-State losses. The average THD value obtained is close to 2.5% which implies power quality enhancement, battery charging efficiency and highlighting the feasibility and adaptability of the proposed system for energy conversion and advanced EV charging station infrastructure development.

Introduction

The usage of Electric Vehicle (EV's) has been increased in recent years which act as suitable alternative transportation instead of using fuel-based vehicles. For past few years, entire world moves towards EVs for mobility due to zero pollution in environment, greenhouse effect and carbon footprints. So, the expansion of Level 3 DC fast charging is essential for EVs which provide a concrete solution to suppress the air pollution and thereby improves the air quality level towards the sustainable healthier environment [1]. Nowadays, government sector comes forwarded to introduce various policies and subsidies for promoting EVs and its charging infrastructure. These kinds of initiatives make us to use e-mobility from fuel-based transportation [2]. Globally, the expansion of fast EV charging unit gets increased every year. As per the statistics, in the year 2024 the fast-charging stations valued around 8.3 billion and then it is expected to reach around 100 billion by the year 2030 [3]. In India, around 40% of the charging stations equipped with fast charger infrastructure which significantly reduce time and cover long distance travel.

The main critical thing in EV based ecosystem is to make ensure providing more energy efficient, reliable and stable charging infrastructure to satisfy the customers. Energy efficient ON-board fast DC Charging stations is getting increases everywhere to meet out the public demand [4]. The advanced smart grid integration with renewable energy provides the better solution for this consistent development in EV charging infrastructures. Government has planned to integrate renewable energy like solar and wind with EV Charging station is very much needed in coastal areas for sustainability and environmental protection.

* Corresponding author.
E-mail addresses: kpsuresheee@gmail.com (S.K. Paramasivam), rameshksrce@gmail.com (R. Senniyappan), senthilkumar.ramu@vit.ac.in (S.K. Ramu), senthilkumar@psgitech.ac.in (S. Mani).

https://doi.org/10.1016/j.rineng.2025.106880
Received 12 June 2025; Received in revised form 8 August 2025; Accepted 20 August 2025
Available online 21 August 2025

Table 1
Preceding affined works: contribution and limitations.

References	Control Approach and contribution	Limitations observed
[5]	A combined wind and grid-powered (CWGP) onshore beach charging station (OSBCS) - comprehensive overview of the feasibility and environmental impact of the charging station	• Lacks analysis on power quality concern and fast charging perspective and THD spectrum
[7]	Bidirectional onboard charging with CLLC resonant converter used with high frequency switch	• Voltage stress more in the high switching operation and cause EMI • Fast charging not applicable • Lacks analysis of Power quality disturbances
[8]	Unit vector control technique used to maintain power quality during fast EV charging with optimization	• Renewable energy sources not used to compensate or inject during power quality issues • Lack of adaptive control techniques like fuzzy • Lacks analysis of THD spectrum
[9]	High gain optimized HGNISUC converter with type-2 fuzzy system to track maximum power point in step-up DC-DC converter	• Lacks voltage balance study in the Load side capacitor • Medium frequency transformer leads to more ON state losses
[10]	Level 3 electric vehicle charging with solar PV along with MPPT controller	• Step-up and Step-down transformer used before rectifier as isolation network which increases complexity of the system • Lacks efficiency analysis of P&O type MPPT used which advanced features of recent tracking system
[12]	Reducing electric vehicle charging impacts on grid through machine learning concepts	• Lack of analyzing the THD spectrum induced in the transmission and distribution system • Lacks analysis of dynamic grid integration and economic considerations
[13]	Solar powered smart charging system contributed with 1) effective load management of EVs 2) real-time monitoring of charging slots at a charging station, 3) smart security system, and 4) integration of renewable energy resources (RERs) into charging stations.	• Lack of integrating other renewable energy sources like wind or biomass • It works under a specific location alone not adoptable for all location and complexity • Lack of analyze power quality disturbances while connecting both slow and fast charging
[16]	Vienna rectifier for EV charging with inherent current control loop in the voltage-oriented control strategy (VOC-VR)	• Lacks current control study to limit harmonics • THD value obtained as 3.25% which is greater than the proposed system
[20]	Grid integrated PV system for EV charging systems with or without BESS for sustainability	• Lacks impact analysis while connecting non-linear load with grid system
[23]	Interleaved 6-level gain bidirectional converter for Level 2 Electric Vehicle charging	• Lack of analysis on off board charging with renewable energy sources
[26]	DC fast charging with high efficient Vienna rectifier for power level more than 15kW	• Complexity and advanced control algorithm are required to operate Vienna rectifier
Proposed Work	**IIPQ controlled Three phase T-Type Vienna Rectifier for High Efficient Off Board Fast EV Charging Station with Enhanced System Stability**	**Due to high switching frequency, non-isolated converter and fast charging current leads to induce significant thermal stress on rectifier switches which require suitable heat sink and safety precautions**

The challenges of renewable energy with grid and its performance analysis were discussed [5].

Ultra-fast EV charging stations always operates in high power rating which imposes nonlinear load on the micro grid. Hence, these loads tend to create PQ issues like voltage sag, voltage swell, total harmonic distortion and reduced reactive power. These kinds of PQ issues will degrade the entire efficiency of the charging unit [6]. Moreover, the bidirectional onboard charging with CLLC resonant converter used with high frequency switch and harmful effects exist on the utility grid leads to systems stability as well as reduce the lifespan of the EV batteries are discussed in reference[7,8].

The solar photovoltaic based charging stations plays vital role in sustainability of the ultra-fast EV charging infrastructure. For sustainability, non-isolated converter plays major role with fuzzy based MPPT techniques involved to achieve higher efficiency. Hence, the solar based public charging stations enhances to decrease the need of conventional fossil fuel-based energy [9]. Moreover, this integration helps to mitigate the CO2 emission and minimize the utility grid voltage stress during peak demand. In India, there is abundant availability of the solar irradiation has more feasibility to develop solar based PV integrated EV charging stations with level 3 rating and it has been monitored with machine learning technique [10,11]. Nowadays, Central government in India has been proposed lot of subsidy scheme under Ministry of New and Renewable Energy (MNRE) to develop efficient and cost-effective based EV charging stations [12]. To improvise these EV charging domain in an effective way, these integration of solar with utility grid becomes more challenges for the researchers, including the requirement of advanced power electronic AC-DC converter, DC-DC converter with effective Power Quality (PQ) Improvement system for energy efficiency. Recent investigation states that the feasibility and energy efficiency of EV charging stations powered by solar energy with enhanced intelligent control technologies. Solar powered smart charging has enabled with real time monitoring system, security system and load management system integrated with renewable energy has discussed in reference [13]. The error deviation and the voltage stress occur in the rectifier unit can be controlled by SAPF along with maintaining constant DC-Link capacitor voltage [14,15].

T-Type Vienna Rectifier (TTVR) provides better solution for addressing all these challenges related to power electronic converter side. It consists of 3 phase – 3 Level 4 Wire rectifier topology to emerges the better efficiency, low switching voltage stress and also consistently maintain stable DC-link voltage [19]. Comparative study of the various EV charging techniques with power quality improvement integrated with active filter provides grid stability while integrate renewable energy. Grid integrated PV system for EV charging systems with or without BESS for sustainability with economic feasibility has been discussed in reference [20]. This proposed TTVR method provides promising solution for the mentioned challenges due to non-linear load and highly suitable for the reactive power compensation and minimize the total harmonic distortion (THD). Shunt Active Filter (SAF) integrated with this TTVR can efficiently reduce the power quality issues like sag, swell, harmonics and reactive power. The combined SAF with solar polar PV system with TTVR based utility grid gives effective solution for EV off-board charging stations [21].

The proposed technique provides the IIPQ theory for the extraction of reference current for harmonic compensation and always maintain balanced load. The IIPQ control technique is used to identify the particular reference current signal and enable the dynamic response during fluctuations. Moreover, this technique ensures to maintain the THD level within the ceiling limit prescribed in IEEE standard i.e less than 5%. In addition to that, the TTVR offers more advantages like maintain system parameters and constant output voltage which provides constant battery charging and improved system reliability [16,18].

In TTVR, the primary challenging issue is maintaining the constant voltage across the dc link capacitor C1 and C2 capacitors. Furthermore, the imbalanced voltage across those two capacitors C1 and C2 leads to

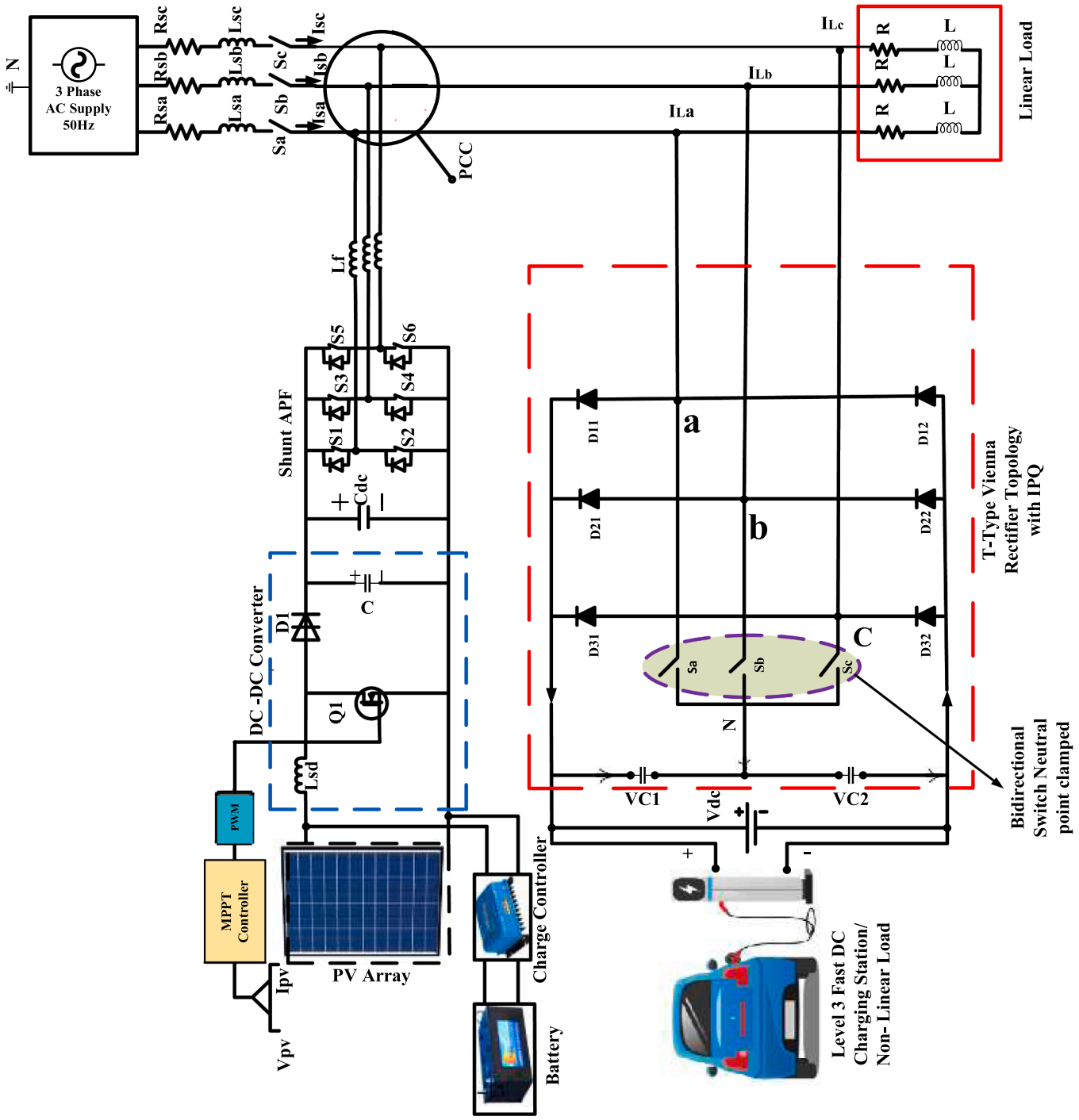

Fig. 1. PV Integrated Shunt APF with T-Type Vienna Rectifier Overview.

inefficient system operation as well as to increase the system complexity [22,23]. To overcome these issues, lot of conventional techniques like Proportional, Proportional- Integral and Proportional-Integral -Derivative controller (P, PI, PID controller) has been already employed, but this methodology is very limited due its inherent system sensitivity and complexity in terms of continuous parameter variations. Hence the optimized control strategies such as Fuzzy Logic Control (FLC) tuned PI controller have been interfaced with this topology to improvise the system performance under dynamic load changing conditions, ensure the precise control of voltage balance at the capacitor C1 and C2 in Vienna rectifier as well as DC-link voltage.

Furthermore, the integrated solar PV system with TTVR based Shunt Active Power Filter (SAPF) provides additional benefits in terms of system stability, energy efficiency and sustainability with reactive power compensation in utility grid. This SPV integrated system is able to operate the grid independently during dynamic or unbalanced load conditions as well as peak hours [24]. During non-linear load conditions exist, the power quality issues occur in power system network which not only create impacts on the charging of EV batteries and also possess the high risk to utility grids stability and its performance. Harmonics leads to system instability, voltage stress, overheating, malfunction of circuit breakers and inaccurate control signals [25]. The proposed system ensures that to suppress the PQ issues and also provides seamless charging control for EV charging customers while maintain utility grid stability.

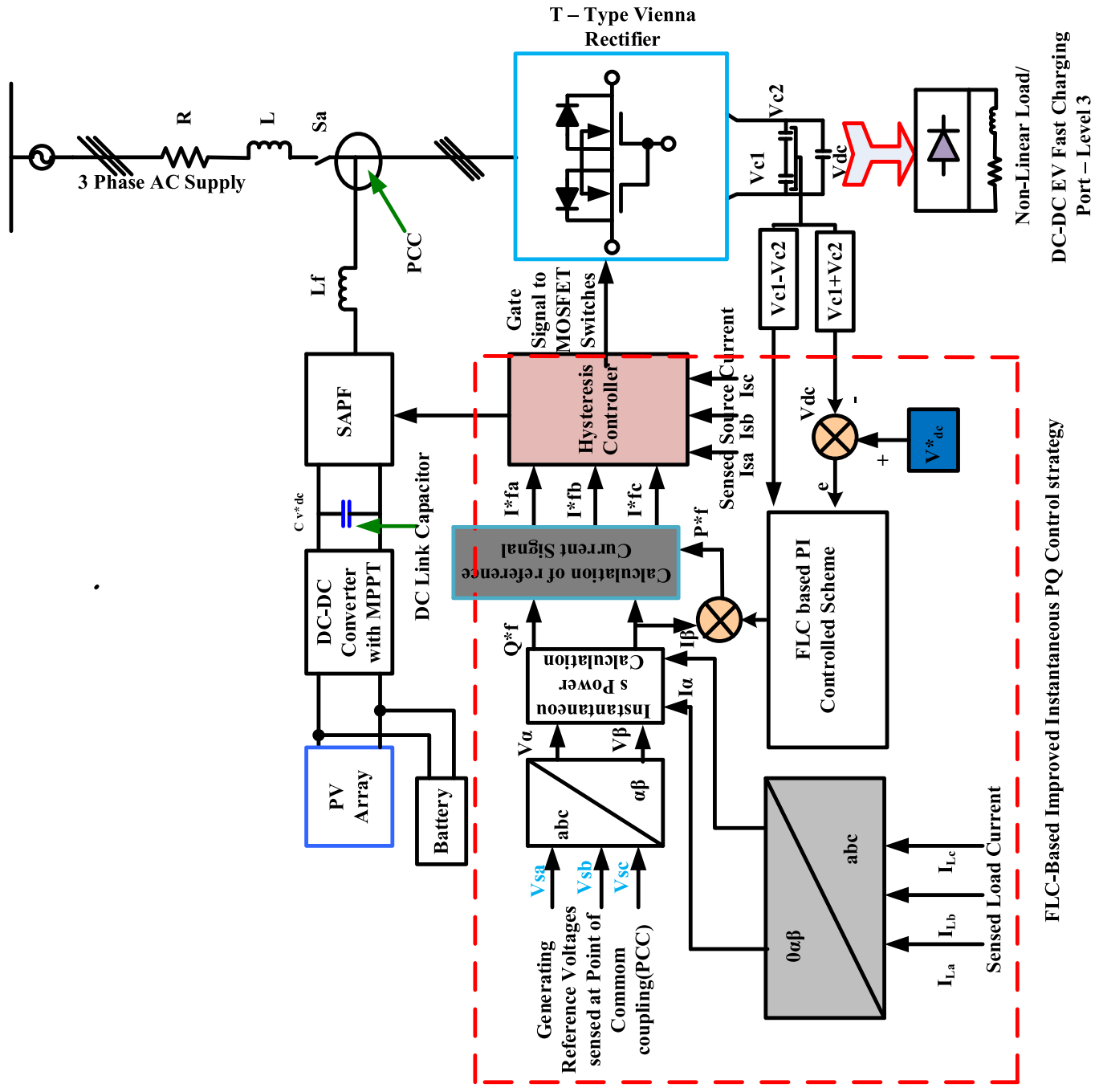

Fig. 2. SPV interfaced SAPF with T-Typer Vienna Rectifier based IIPQ Control Topology.

Finally, the solar PV based TTVR system with Instantaneous real and reactive power (IPQ) control topology represent the significant recent advancement in EV charging infrastructure. It has ability to represent the PQ issues and considered as the modern technology for the EV charging infrastructure. The proposed system not only employs the system reliability and efficiency of the OFF-board EV charging but also pays attention to reduce greenhouse gas emission and highly promote the renewable energy usage. The results obtained from simulation and experimental prototype demonstrates that the suggested methodology has better performance for EV charging and harmonic compensation. The findings show the real time implementation and effectiveness of the IPQ control topology in level 3 charging point.

Literature review on preceding affined works with its contributions and limitations:

Table 1 shows all relevant control approach and its contribution of the already existing works has been discussed along with limitations and proposed work limitations also discussed at the bottom.

In EV charging, there are three levels of charging techniques available as per the requirement of rate of charging of battery with respect to time i.e level 1,2 and 3 based on output power. Based on output power rating, the level 1 charging stations delivers < 5 kilo Watts which is suitable for residential charging purpose. A Level 2 charging station delivers power < 25 kilo Watts which is more suitable for light vehicle charging points at public points [17]. A Level 3 fast DC charging can deliver above 25 kilo Watts which is suitable for commercial purpose. Moreover, onboard charging units is highly suitable at level 1 and 2 charging point, which can adoptable in vehicle (bike/car) itself. Level 3 charging is only suitable at OFF board charging unit, not directly

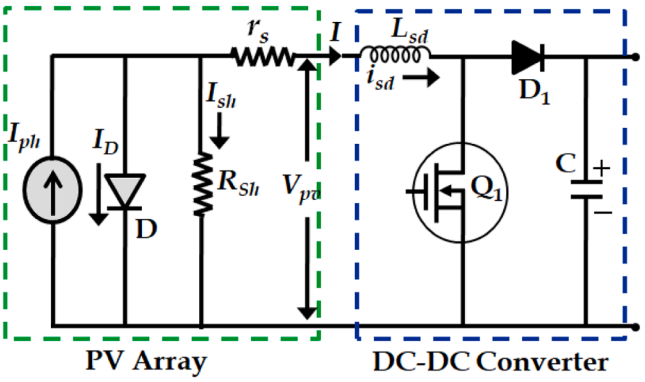

Fig. 3. SPV Cell Equivalent circuit with DC-DC power converter.

connected in vehicle [26]. In this proposed system, TTVR is used for AC-DC power conversion and it is recommended for DC fast charging.

The main objective of this paper is to design an energy efficient OFF board EV charging with TTVR based IIPQ control strategy. In this approach, it mainly focuses to

- Design and development of simulation and controller design of DC-fast EV charging station using 3P3L4W (Three Phase 3 Level 4 Wire System) TTVR for grid to vehicle.
- Improved Instantaneous real power (P) and Reactive Power (Q) – IIPQ control strategy is implemented to extract reference current signal for injecting compensation current at source side.
- SPV power generation integrated with DC-DC step-up converter employed in this method to make the utility grid as stable and maintain power factor.
- Adaptive Fuzzy Logic Controller (FLC) based DC voltage regulator is used to maintain constant DC-Link voltage and balanced voltage at both VC1, VC2 as same at rectifier side for fast charging and energy conversion.

The paper consists of four sections as followed: section 2 deals about the system overview along with schematic diagram of the proposed TTVR based SAPF, SPV system operation with DC-DC power converter and different mode of TTVR operation. Section 3 deals with the mathematical analysis, design of Fuzzy tuned PI Based IIPQ Control Topology for reference line current generation and pseudo code for SPV interfaced IIPQ controlled Vienna rectifier for fast EV charging station details were discussed for easy understanding. Section 4 deals with simulation results and discussion with three different cases. Section 5 deals with experimental analysis to validate the proposed system under different load conditions. Conclusion and future scope of this proposed work are given in last portion.

System description

Energy Efficient OFF Board T-Type Vienna Rectifier for fast EV Battery charging stations with Solar PV based Shunt Active Filters as shown in Fig.1. In this schematic diagram, the Improved instantaneous real and reactive power (IIPQ) controlled technique is employed to excerpt the basic fundamental parameters in load side. This topology extracts the load side as well as source side current value and provides suitable compensation value and generate appropriate PWM signal to maintain system stability. SAPF with Fuzzy based TTVR is able to maintain the DC-DC Link voltage as constant for balancing the capacitor voltage VC1 and VC2. Here, the SAPF act as effective role to suppress the THD level. During peak load hours, the grid supply gets oscillated due to non-linear load and power quality disturbances. To overcome these issues, the solar PV based MPPT controller and battery-based charge controller system is used to compensate the power oscillations in utility grid. Moreover, the SPV system generated excess energy means, it can be stored in battery for further usage. Whenever the SPV energy generation becomes low due to irradiation, the stored energy in battery is utilized to make stable DC link voltage. The power electronic MOSFET based power converter is utilized to improve the PV side voltage by adjusting D value (Duty cycle). The SAPF with filter inductor is connected to utility grid at PCC. In this schematic diagram, the three phase T-Type Vienna rectifier with bidirectional neutral point clamped switch followed by the fast-charging OFF board point is considered as non-linear load. The utility grid can be isolate from this system with the help of three main switches *Sa, Sb* and *Sc* during any maintenance or faulty conditions.

In proposed topology, the reference voltage V* dc and the capacitor balanced voltage in TTVR is identified and compared with the comparator in fuzzy logic unit. The Instantaneous reference current signal generation produce any error signal due to fluctuations in load, then it provides appropriate reference current signal to maintain the grid stability to overcome harmonic issues. Fig. 2 shows SPV interfaced SAPF with T-Typer Vienna Rectifier based IIPQ Control Topology.

Solar Photovoltaic Power generating module with MPPT based DC-DC step up converter

A practical PV cell equivalent circuit diagram with DC- DC Step-up Converter is shown in Fig. 3. It consists of current source parallel to single diode-D, series resistance (r_s) and shunt resistance (R_{sh}). The output characteristics depends upon the solar irradiation level in the environment.

The mathematical relation between current and voltage based in this electrical circuit are shown in the equation given below. The Eq. (1), as shown below, is obtained by based on applying KCL.

$$I = I_{ph} - I_D - I_{sh} \tag{1}$$

Let, I_D denotes the diode current, the photocurrent denoted by I_{ph}, current flows in shunt resistor is denoted by I_{sh} and I denotes PV cell current. The diode current I_D can be expressed by the Eq. (2)

$$I_D = I_0\left(e^{\left(\frac{V+r_sI}{aV_T}\right)} - 1\right) \tag{2}$$

The PV current is derived by the Eq. (3)

$$I = I_{ph} - I_0\left(e^{\left(\frac{V+r_sI}{aV_T}\right)} - 1\right) - \frac{V+r_sI}{R_p} \tag{3}$$

Then, the diode Thermal Voltage V_T is determined by

$$V_T(V) = \frac{n_s kT}{q} \tag{4}$$

SPV array is developed with series modules N_S as well as parallel modules N_P, then the SPV array V-I characteristic is expressed by the following equations

$$I_{pv} = N_p I_{ph} - N_p I_0\left(e^{\left(\frac{V_{pv}+R_{se}I}{N_s aV_T}\right)} - 1\right) - \frac{V_{ph}+R_{se}I_{pv}}{R_{pe}} \tag{5}$$

$$R_{se} = \frac{N_s r_s}{N_p} \tag{6}$$

$$R_{pe} = \frac{N_s R_p}{N_p} \tag{7}$$

k – Boltzmann's constant value (1.3806×10^{-23}J/K), T - operating temperature level (K), q - Electron charge (1.602×10^{-19}C), I_0- Output current at saturation level, V_{pv}-Terminal voltage of PV cell (V),I_{pv}-PV cell

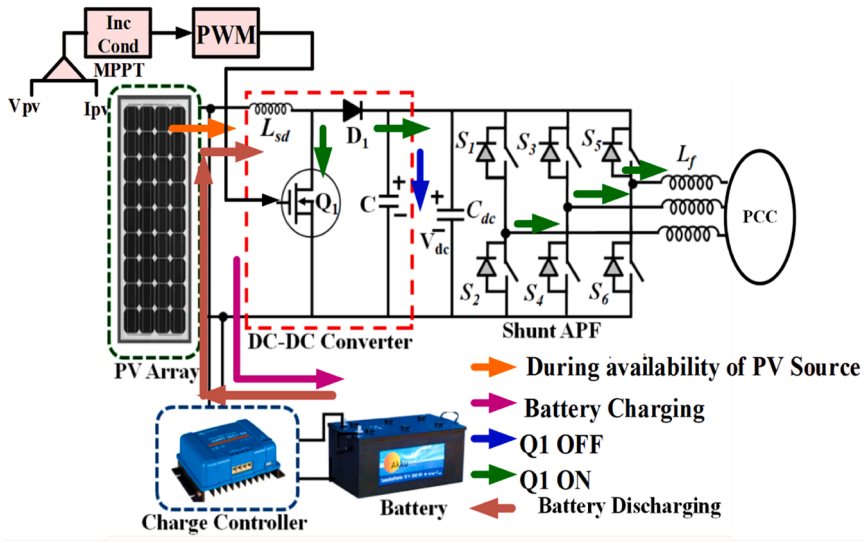

Fig. 4. Three cases of SPV Power compensating modes.

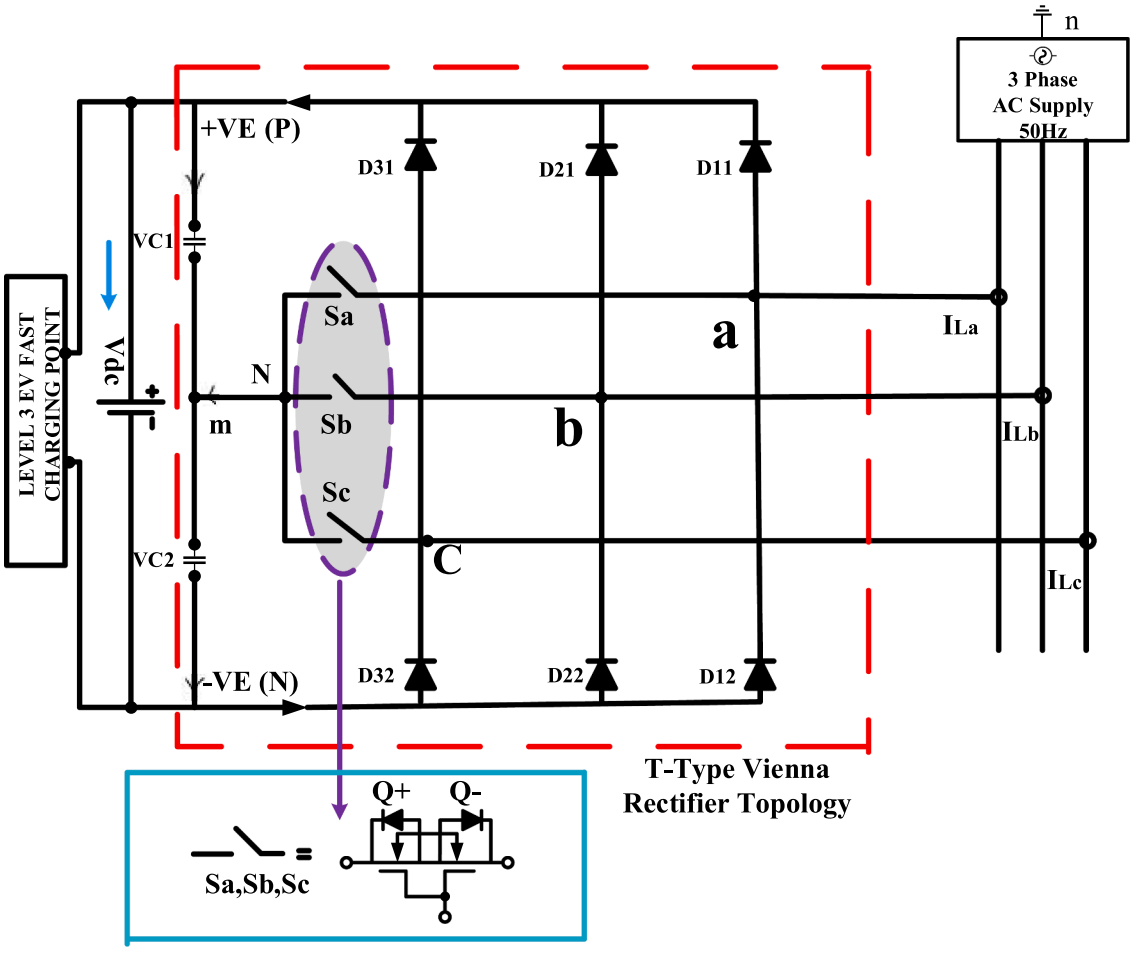

Fig. 5. T Type Vienna Rectifier Schematic Diagram.

photo current (A). Based on the above analysis, the sufficient SPV generated power is given to DC-DC converter with Incremental Conductance based (InC) MPPT controller for obtaining maximum power. Battery with energy management is connected for excess energy storage and discharge whenever is needed to make the utility grid as stable.

Various operating mode of solar photovoltaic power generating system

Fig. 4 depicts that, SPV integrated with DC-DC step-up converter employed in this method. Here, the Vspv represents the SPV voltage generated, Tswp is switching time period of MOSFET, ΔIL is change in current ripple of inductor Lsd, ΔVc is capacitor change in ripple voltage

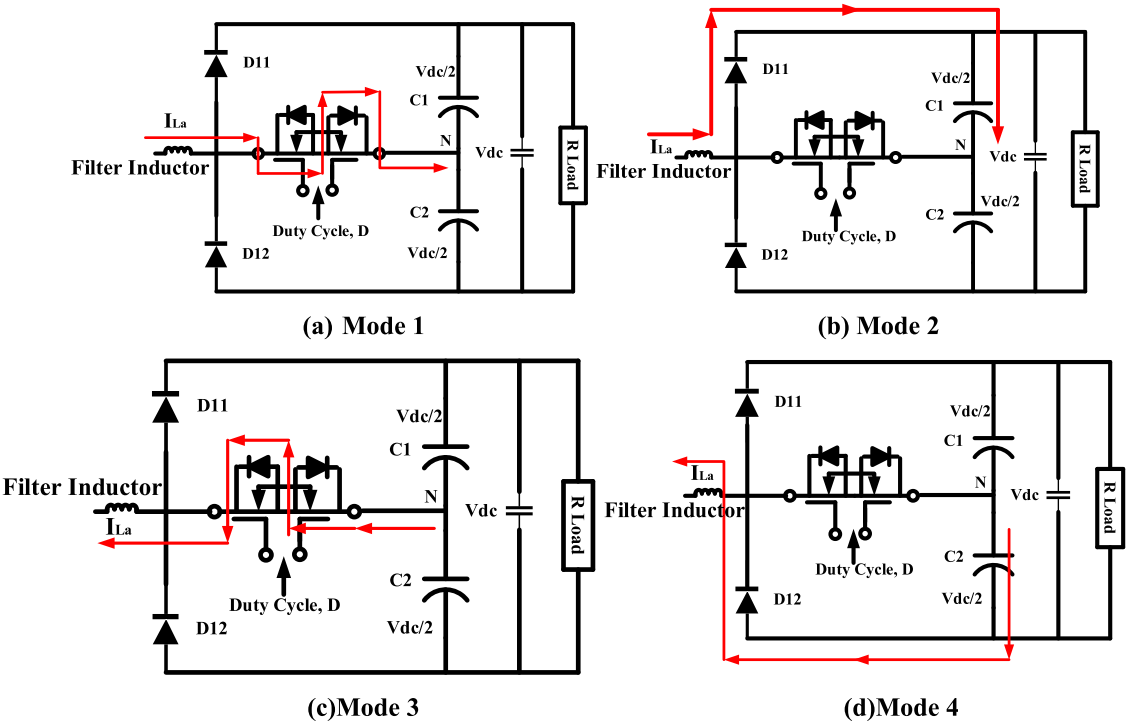

Fig. 6. TTVR- PWM Modulation Scheme at A Phase.

Table 2
Different switching states and produced pole voltages of Vienna rectifier.

S. No	Operating State	S1	S2	S3	Pole Voltages		
					VaM	VbM	VcM
1	+VE	OFF	OFF	OFF	+Vdc/2	-Vdc/2	-Vdc/2
2	+VE	OFF	OFF	ON	+Vdc/2	-Vdc/2	0
3	+VE	OFF	ON	OFF	+Vdc/2	0	-Vdc/2
4	+VE	OFF	ON	ON	+Vdc/2	0	0
5	-VE	ON	OFF	OFF	0	-Vdc/2	-Vdc/2
6	-VE	ON	OFF	ON	0	-Vdc/2	0
7	-VE	ON	ON	OFF	0	0	-Vdc/2
8	M	ON	ON	ON	0	0	0

and *rs* is the series resistance in DC-DC converter. Hence the relation between inductor, capacitor and duty cycle is represented as (Inductor, L= D.Vspv.Tswp / ΔIL) and (Capacitor, C= D.Vo.Tswp / rs.ΔVc). MOSFET switch receives the control signal from MPPT controller via PWM pulses as duty cycle, D. When Q1 turns to ON, the inductor (Lsd) gets charged by SPV module. When Q1 turns to OFF, the SPV generated energy can store in battery as well as feed to the inverter through diode, D1. The OFF Board TTVR fast EV Battery charging stations with SPV based Shunt Active Filters operate under three different cases to compensating the utility grid current disturbances at source side. Three cases such as compensation with SPV generation alone, compensation with SPV generation as well as battery charging mode and compensation with battery backup source during unavailability of solar power. Fig. 4 shows the current flow direction of SPV power generation for all these three above mentioned cases.

Four working states of TTVR: mode of operation

T Type Vienna rectifier plays major role in all power conversion sectors due to its practical feasibility and effectiveness in addressing the PQ issues and maintain the system as sustainable. Fig. 5 shows the schematic structure of 3L3S-TTVR used in fast EV charging station. Filter inductance, L and equivalent resistance, R of 3 phase AC source side is connected with bidirectional switch Sa, Sb, Sc. Another end of switches is connected to the neutral point at DC charging side. Each TTVR switch consist of two bidirectional MOSFET switch with two diodes and capacitors VC1 and VC2. The main advantage of this topology is to maintain smooth input supply to the charging unit without any switching voltage stress and suppress the higher odd order harmonics. TTVR is working in four modes at various load conditions. This control topology maintains balanced voltage in both the capacitors at VC1 and VC2 as well as reduce the DC side voltage ripples.

In an OFF-board EV Charging stations with ranges between 15KW to 20 KW get the input 3 phase AC power supply from utility grid and then it is converted to DC. Even though many existing topologies available for this power conversion, this proposed TTVR is more popular nowadays due to its continuous conduction mode of operation, reduced switching and voltage stress with reduced number of switches. In this proposed system, the hysteresis current controller (HCC) has been implemented to generate PWM gate pulse for TTVR. Fig. 6 shows the TTVR- PWM Modulation Scheme at any one phase (A-Phase). The switching action is controlled by the duty cycle, D which is provided to PWM module. The proposed TTVR consist of 4 switches in each leg (2 diodes and 2 MOSFET) and all the 3 phases (A, B, C) is commonly connected at neutral point N. At mode 1, the switch S1 is ON during +VE current flow at load side, the pole voltage value is equal to zero at mid-neutral point M. At mode 2, the current maintains same +VE direction but the Switch S1 is OFF, then current redirect through diode D11, then the rectifier operates in positive state which generates pole voltage is equal to + Vdc/2. At mode 3, the switch S1 is ON state, the current flow is -VE, then the generated pole voltage value is equal to zero. At mode 4, the current maintains same -VE direction, but switch S1 in OFF state, then current redirect through diode D12, then the pole voltage becomes -Vdc/2. Hence, the remining B and C phases works same as like these produced pole voltages and different switching states of phase A. Table 1 shows

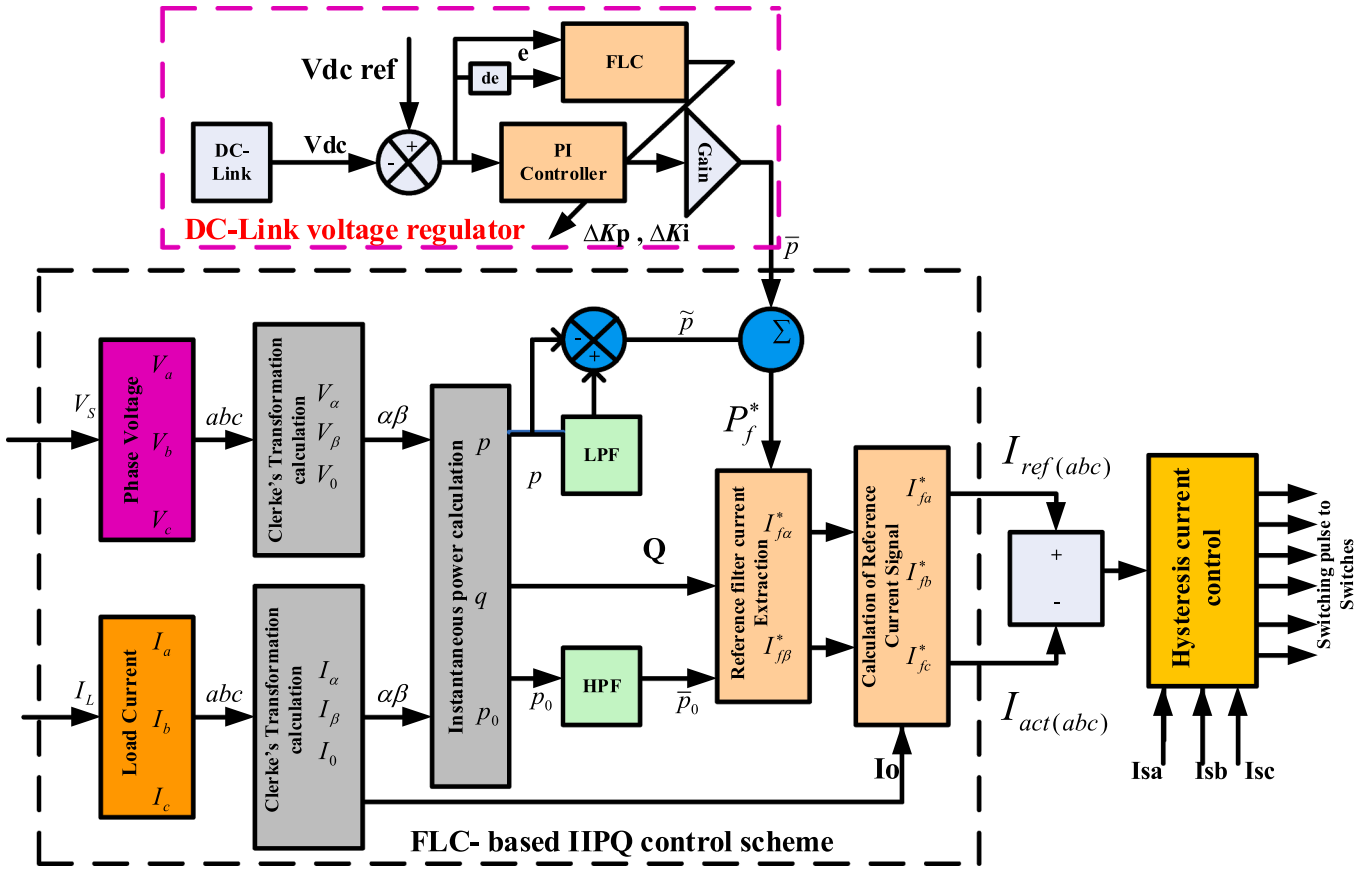

Fig. 7. Schematic diagram of Fuzzy tuned PI based IIPQ Control strategy.

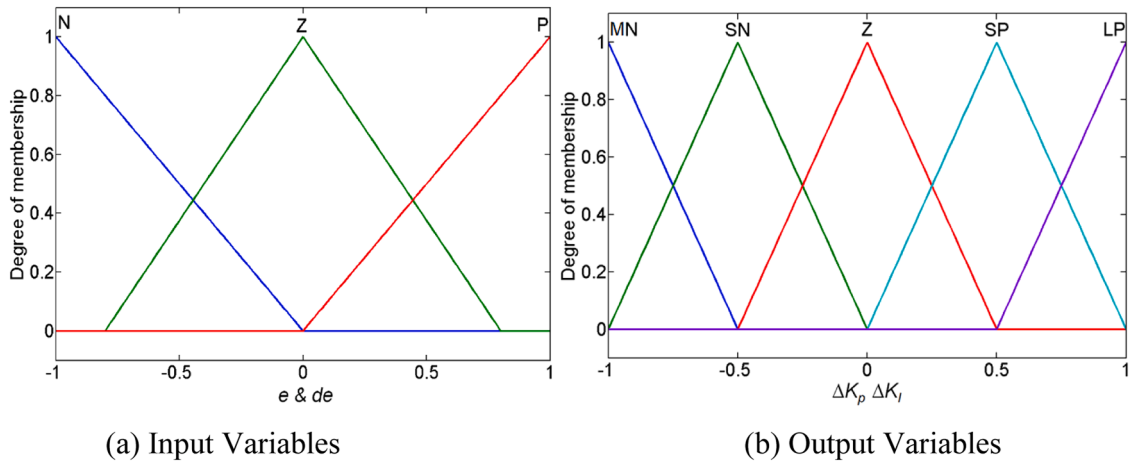

Fig. 8. Membership function for input and output variables.

Table 3
Fuzzy decision rules.

e / *de*	N	Z	P
N	MN	SN	Z
Z	SN	Z	SP
P	Z	SP	MP

the different switching states of three phase three level VR with produced pole voltage at various operating point.

Here, the various combinations of switching operations in the TVVR can produce pole voltage VaM, VbM and VcM at the mid point (M) per phase leg has connected with +Ve terminal (P), and -Ve terminal (N). As per the data mentioned in Table 2 shows the various switching combinations produce three level (+ Vdc/2, 0, -Vdc/2) as line-line voltage.

2.4. Design and modeling of TTVR

AC side expression expressed by the Eq. (8)

$$E = L\frac{dI}{dt} + R_I + V \tag{8}$$

Where the 3 phase voltages(E) is expressed as Ea, Eb and Ec.

Table 4
Pseudo code for SPV interfaced IIPQ controlled Vienna rectifier for fast EV charging station.

```
BEGIN
Step 1:  Measure System Parameters
         Measure Vpv, Ipv from Solar Photovoltaic panel
         Measure Vs_abc, Is_abc, IL_abc from grid // From source side and load side
Step 2:  Perform MPPT using Incremental Conductance (INC) Method
         IF (dIpv/dVpv == -Ipv/Vpv)
           Maximum Power Point (MPP) reached and maintain constant duty ratio
         ELSE
         Adjust duty ratio D to track MPP
Step 3:  Control DC-DC Converter for maintain DC-Link voltage stable
         Regulate Vdc using D
Step 4:  Compute Improved Instantaneous Power Real and Reactive (P&Q)
Step 5:  Clarke Transformation
         [α, β] = Clarke_Transform(IL_abc)
Step 6:  Generate Instantaneous Reference Current signal using adaptive Fuzzy PI Controller
         e = Iref - IL
         de = Derivative(e)
         Iref_αβ = Fuzzy_PI_Controller(e, de)
Step 7:  Inverse Clarke Transform to get Iref_abc
         Iref_abc = Inverse_Clarke_Transform(Iref_αβ)
Step 8:  Hysteresis Current Control
           IF IL > Iref_abc + Band THEN
             Turn OFF corresponding switch
           ELSE IF IL < Iref_abc - Band THEN
             Turn ON corresponding switch
           END
Step 9:  Generate Gate Pulses to rectifier and converter
Step 10: Harmonic Analysis and Compensation
         SWITCH system_condition:
  CASE 1: Balanced input + balanced/static load // Minimal compensation needed
           Skip harmonic injection
  CASE 2: Balanced input + nonlinear load
  CASE 3: Unbalanced input + nonlinear load
Step 11: Maintain balanced Stable Voltage at Vdc = Vc1 + Vc2
         IF |Vdc - Vref| ≤ Ripple_Tolerance THEN
           Maintain stability
         ELSE
           Adjust control parameters to restore Vdc
         END
```

Table 5
Component details considered for FLC based IIPQ control topology.

S. No	Hardware Components Description with Range
1	Phase Voltage – 230 V
2	Utility Grid Frequency – 50 Hz
3	Total Harmonic Distortion, iTHD <5% (IEEE Std)
4	DC-Link Voltage – 520 V
5	DC-Link Capacitor - 2800 μF
6	Filter Inductor – 38 μH
7	SiC MOSFET Switch - IRFP260
8	Switching Frequency – 20 kHz
9	Feeder Impedance rating - 1+j3.167 Ω
10	PV array Short Circuit Current – 8.65 A
11	PV array Open Circuit Voltage - 44 V
12	PV array Impp – Current - 8.21 A
13	PV array Vmpp – Voltage - 36 V
14	Solar Irradiation - 1000 W/m2
15	Proportional Coefficient, Kp = 4
16	Integral Coefficient, Ki = 0.3
17	DC - DC Converter –(Ls-0.715μH, C - 320μF)
18	Non-Linear load R_L -20 Ω, L_L - 0.5mH
19	Diode Rectifier (L_L.3mH, L_{DC} - 5.7mH, R_{DC} .12 Ω)
20	Battery – 48V, 500 Ah

$$E_a = E_m \cos(\omega t) \tag{9}$$

$$E_b = E_m \cos\left(\omega t - 2\frac{\pi}{3}\right) \tag{10}$$

$$E_c = E_m \cos\left(\omega t + 2\frac{\pi}{3}\right) \tag{11}$$

In Eq. (9), (10) and (11), Em denotes the amplitude of voltage in each phase. The phase voltages can be expressed as V_{an}, V_{bn}, V_{cn} in Eq. (12), (13) and (14).

$$V_{an} = V_{am+} V_{mn} \tag{12}$$

$$V_{bn} = V_{bm+} V_{mn} \tag{13}$$

$$V_{cn} = V_{cm+} V_{mn} \tag{14}$$

In DC side, the capacitor voltage V_{C1} and V_{C2} generates the error voltage, V_e when those two capacitor voltages become unbalanced. Moreover, the voltage error occurs due to the mid-point neutral current I_m. The voltage error V_e can identified from the difference between both the voltage at capacitor C1 and C2. Eq. (15) depicts the identification of error voltage at dc-side capacitor.

$$I_m = C1\frac{dV_{C1}}{dt} - C2\frac{dV_{C2}}{dt} = C\frac{dV_e}{dt} \tag{15}$$

The main objective of the proposed TTVR is regulation of the DC-link voltage, control of line current during dynamic conditions and reactive power compensation.

In the proposed system, the V_{dc} value can be considered based on the below Eq. (16).

$$V_{dc} = \frac{2\sqrt{2}V_{LL}}{\sqrt{3}(M)} \tag{16}$$

Here, V_{dc} voltage value is always maintained greater than the Line to Line (L-L) voltage. So, consider the L-L voltage as 320V and Modulation Index Value as unity. Hence, the V_{dc} becomes 522.5V which is approximately taken as 520V. Design value of capacitor, C_{dc} can be identified from the Eq. (17) and the DC-Link capacitor value obtained is 2797.51 μF and it is taken as 2800 μF as per the calculation with below values.

$$C_{dc} = \frac{6V_{ph}\alpha I_{ph}t}{\left(V_{dcref}^2 - V_{dc}^2\right)} \tag{17}$$

Where,

Actual DC voltage $V_{dc} = 510$ V, Reference DC voltage, $V_{dcref} = 520$ V, Phase Voltage $V_{ph} = 230$ V, Current $I_{ph} = 58$ Amp, Constant Loading Factor $\alpha = 1.2$,Time taken, $t = 300$ μs

3. Design of Fuzzy tuned PI Based IIPQ Control Topology for reference line current generation

The schematic diagram of the generation of the reference line current generation that are used by T-Type Vienna Rectifier for fast EV Battery charging stations with adaptive FLC tuned PI based control scheme as shown in Fig. 7. The objective of this topology is to stabilize the utility grid supply without any harmonics and identify the fundamental basic load side parameters and compute it on to the source side. Here, Clarke transformation is used to transform the source side voltage and current into Voαβ coordinates and Ioαβ . The dc side voltage regulation and current compensation takes place here before supplying rectifier unit.

The schematic diagram of the FLC tuned current reference signal generation by using Clark transformations as shown in Fig. 7. The phase voltage (Va, Vb, Vc) and load side current as (Ia, Ib, Ic) are measured and converted to $V_{0\alpha\beta}$ and $I_{0\alpha\beta}$. Eqs. (18) and (19) shows the zero-sequence voltage and current with the pole axis voltage and current respectively in Clarke's transformation pattern.

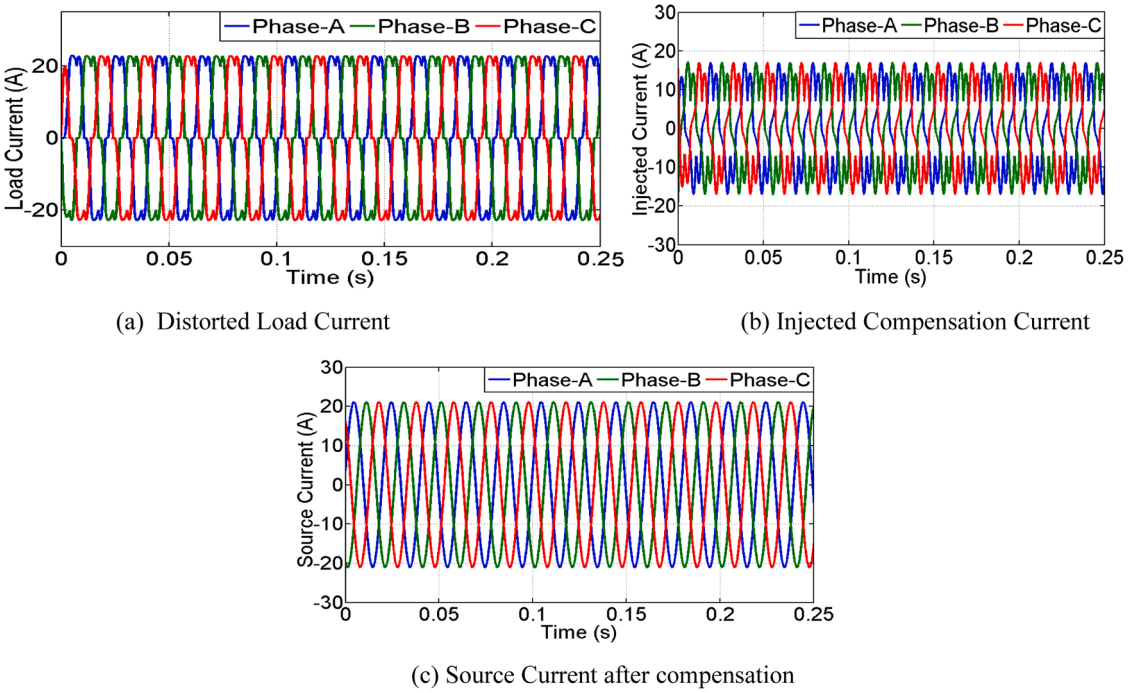

Fig. 9. (a) Distorted Load Current (b) Injected compensation current (c) Source current after compensation.

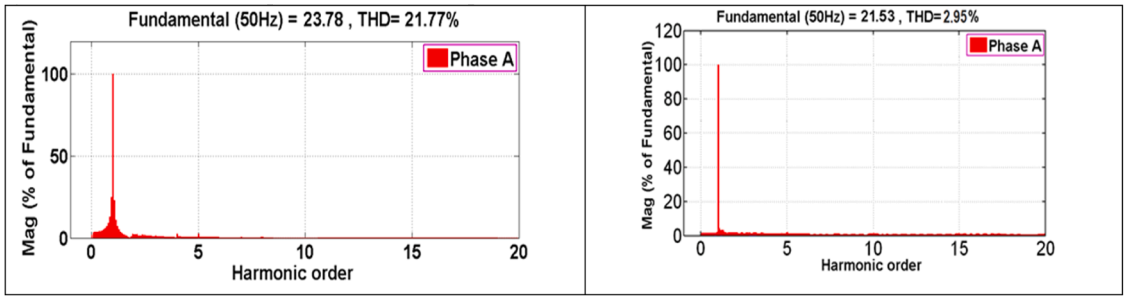

Fig. 10. Spectral analysis of THD – before and after compensation.

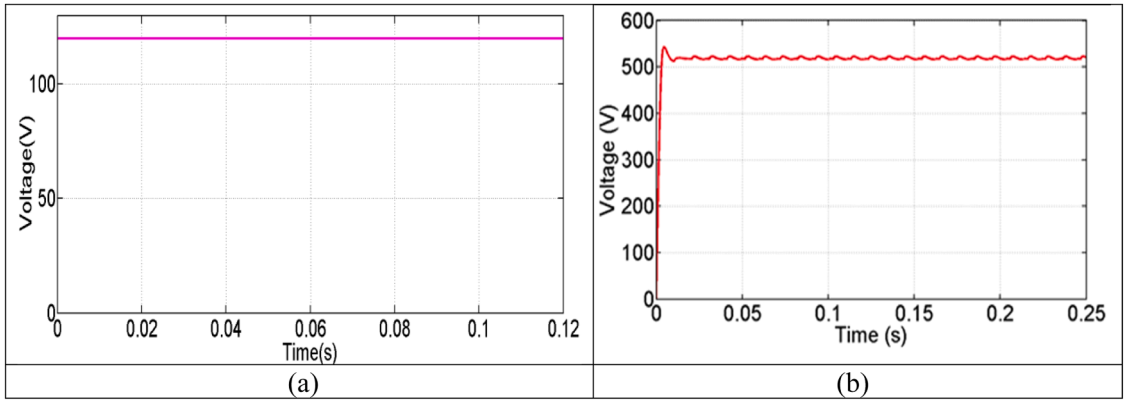

Fig. 11. (a) PV array voltage (b) DC-Link voltage.

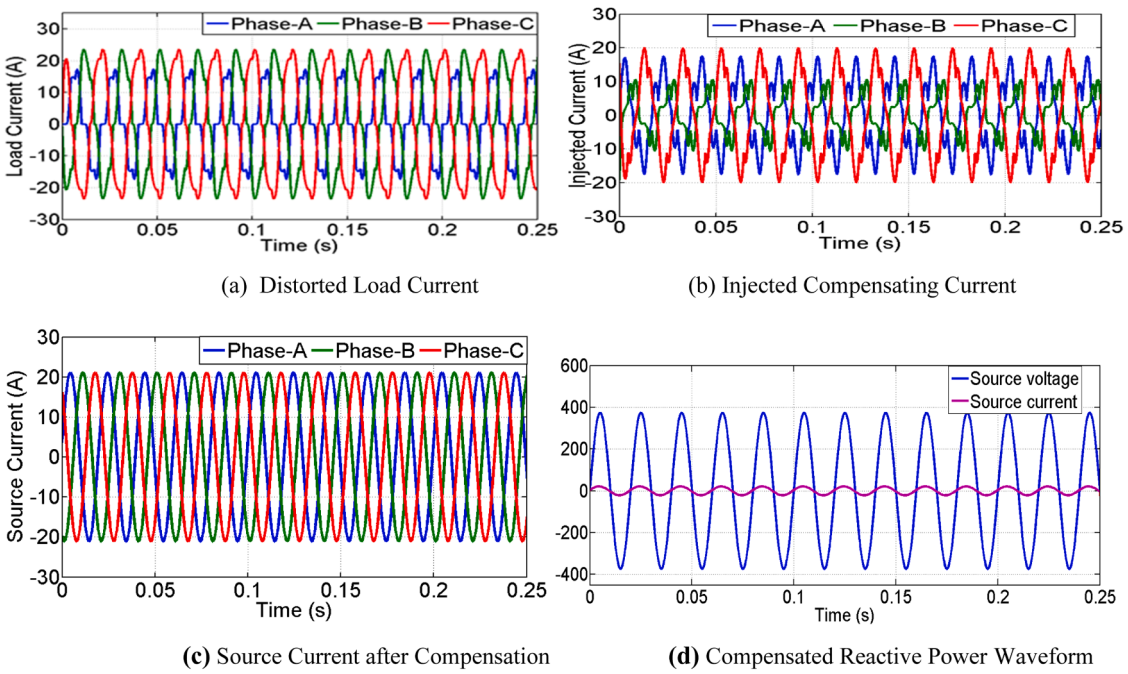

Fig. 12. (a) Distorted load current (b) Injected compensating current (c) Source Current after Compensation (d) Compensated Reactive Power Waveform.

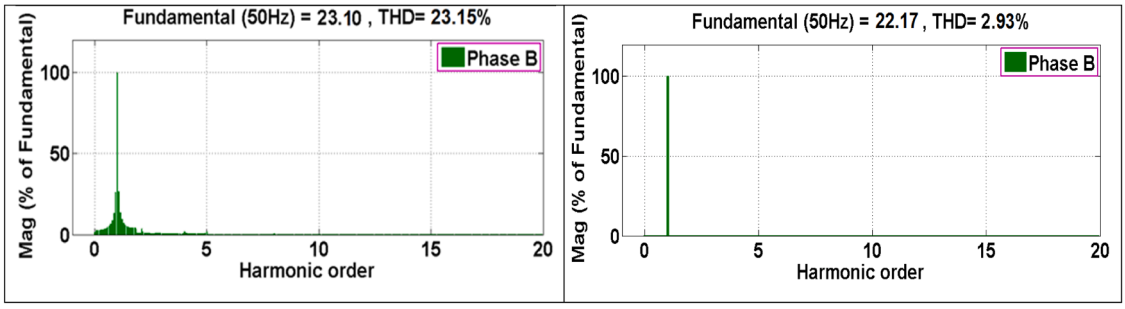

Fig. 13. Spectral analysis of THD for before and after compensation.

$$\begin{bmatrix} V_0 \\ V_\alpha \\ V_\beta \end{bmatrix} = \sqrt{\frac{2}{3}} \begin{bmatrix} \frac{1}{\sqrt{2}} & \frac{1}{\sqrt{2}} & \frac{1}{\sqrt{2}} \\ 1 & -\frac{1}{2} & -\frac{1}{2} \\ 0 & \frac{\sqrt{3}}{2} & -\frac{\sqrt{3}}{2} \end{bmatrix} \begin{bmatrix} V_a \\ V_b \\ V_c \end{bmatrix} \tag{18}$$

$$\begin{bmatrix} I_0 \\ I_\alpha \\ I_\beta \end{bmatrix} = \sqrt{\frac{2}{3}} \begin{bmatrix} \frac{1}{\sqrt{2}} & \frac{1}{\sqrt{2}} & \frac{1}{\sqrt{2}} \\ 1 & -\frac{1}{2} & -\frac{1}{2} \\ 0 & \frac{\sqrt{3}}{2} & -\frac{\sqrt{3}}{2} \end{bmatrix} \begin{bmatrix} I_a \\ I_b \\ I_c \end{bmatrix} \tag{19}$$

The real (active) and imaginary (reactive) power can be expressed as P and Q in Eq. (20) as matrix form. Here the Instantaneous power flow as well as energy exchanged between two phases as represented.

$$P = V_\alpha I_\alpha + V_\beta I_\beta$$

$$Q = V_\beta I_\alpha - V_\alpha I_\beta$$

$$\begin{bmatrix} P \\ Q \end{bmatrix} = \begin{bmatrix} V_\alpha & V_\beta \\ V_\beta & -V_\alpha \end{bmatrix} \begin{bmatrix} I_\alpha \\ I_\beta \end{bmatrix} \tag{20}$$

Here the harmonic effect in the active and reactive component are reduced by using low pass filter and high pass filter to obtain exact value of P. The summation of average value of power loss ($\bar{p}$) and oscillatory component ($\tilde{p}$) provides actual power flow (P_f^*) which is actually needed to maintain the DC-Link voltage as constant. The average value of power loss and oscillatory components in terms of three phase load current is expressed in Eq. (22).

$$P_f^* = \bar{p} + \tilde{p} \tag{21}$$

$$\bar{p}_L + \tilde{p}_L = \begin{bmatrix} \bar{p}_{La} \bar{p}_{Lb} \bar{p}_{Lc} \end{bmatrix} + \begin{bmatrix} \tilde{p}_{La} \\ \tilde{p}_{Lb} \\ \tilde{p}_{Lc} \end{bmatrix} \tag{22}$$

The reference filter current signal is expressed in Eq. (23) and (24)

$$I_{f\alpha}^* = \left[\left(\frac{-1}{V_\alpha^2 + V_\beta^2} \right) \left(\left(P_f^* + V_\alpha \right) + \left(Q + V_\beta \right) \right) \right] \tag{23}$$

$$I_{f\beta}^* = \left[\left(\frac{-1}{V_\alpha^2 + V_\beta^2} \right) \left(\left(P_f^* + V_\beta \right) - \left(Q + V_\alpha \right) \right) \right] \tag{24}$$

The proposed adaptive FLC- tuned PI based DC-Link voltage regulator ensures the active closed-loop control strategy by fuzzy based PI controller tuning process. In this system, the input signals (e - error) and

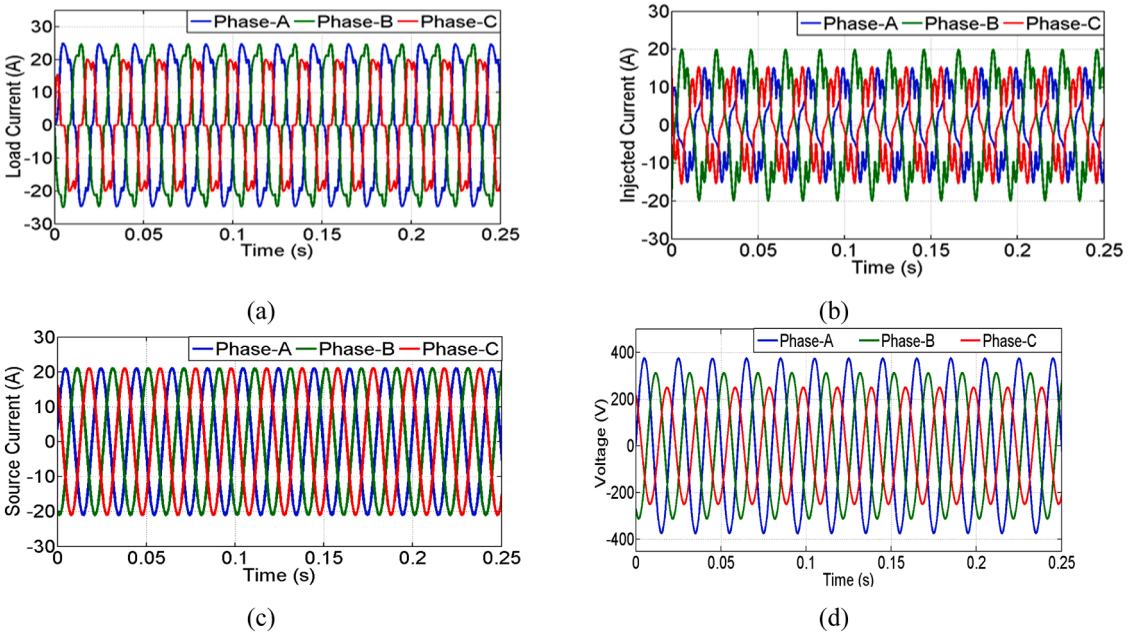

Fig. 14. (a) Distorted load current (b) Injected current for compensation (c) Source current after compensation (d) Unbalanced supply voltage.

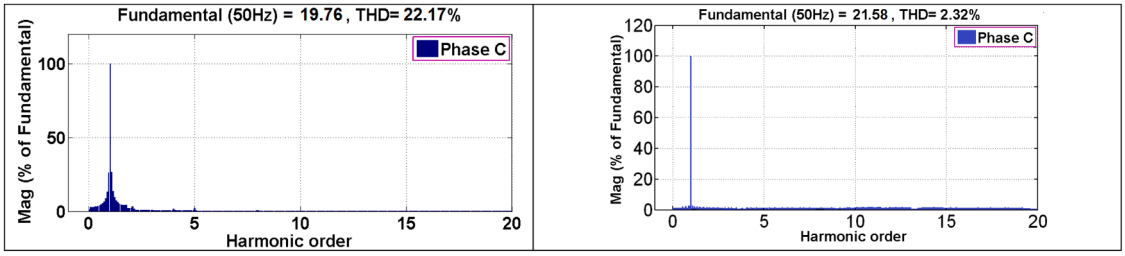

Fig. 15. Speshows the spectral analysis of THD for before and after interface ctral analysis of THD for before and after IIPQ control stratergy.

(de – change in error) will get regularized with scaling factors. The fuzzy based inference engine process fuzzification, rule based logical decision followed by defuzzification. Based on the input signals, the system determines the outputs of the fuzzy controller as ΔKP, ΔKI value required for PI controller tunning purpose. Here the fuzzy subset has been separated into three different input variable values as positive (P), negative (N) and zero (Z) and the five different output variable values as Maximum Negative (MN), Small Negative (SN), Zero (Z), Small Positive (SP) and Maximum Positive (MP). Fig. 8 shows the input and output variables as membership function. Here, the maximum positive to maximum negative methodology was implemented in this fuzzification approach to convert exact equivalent variables. Table 3 shows the fuzzy decision rules.

Based on above said rules, the regulated power can be obtained through PI controller as per Eq. (25)

$$P_{reg=} K_p\, e + K_I \int e\, dt \tag{25}$$

Let, the gain values of K_p and K_I are derived by the following Equations.

$$K_p = K_{P0} - \Delta K_p \tag{26}$$

$$K_I = K_{I0} - \Delta K_I \tag{27}$$

Let, the self-tuned PI parameters is obtained as by estimate this function of error,e and change in error value de as given in Eqs. (28) and (29) respectively.

$$\Delta K_p = f_1(e, de) \tag{28}$$

$$\Delta K_I = f_2(e, de) \tag{29}$$

Hence, the reference current I^*_{fa}, I^*_{fb}, I^*_{fc} signals are calculated with Clarke's transformation methos expressed in the Eq. (30).

$$\begin{bmatrix} I^*_{fa} \\ I^*_{fb} \\ I^*_{fc} \end{bmatrix} = \sqrt{\frac{2}{3}} \begin{bmatrix} \frac{1}{\sqrt{2}} & \frac{1}{\sqrt{2}} & \frac{1}{\sqrt{2}} \\ 1 & -\frac{1}{2} & -\frac{1}{2} \\ 0 & \frac{\sqrt{3}}{2} & -\frac{\sqrt{3}}{2} \end{bmatrix} \begin{bmatrix} I^*_{f0} \\ I^*_{f\alpha} \\ I^*_{f\beta} \end{bmatrix} \tag{30}$$

Pseudo code for IIPQ control three phase vienna rectifier for fast EV charging station with enhanced system stability

This section deals with the pseudo code for IIPQ Controlled Three Phase Three Level Four Wire T-Type Vienna Rectifier for Highly Efficient Off Board Fast EV Charging Station with Enhanced System Stability in step-by-step flow from begin to end. Table 4 shows the line-by-line steps involved in the proposed system for easy understanding how it works.

Results and discussion with various load conditions at electric vehicle charging station

Energy efficient OFF board grid connected T-Type Vienna Rectifier

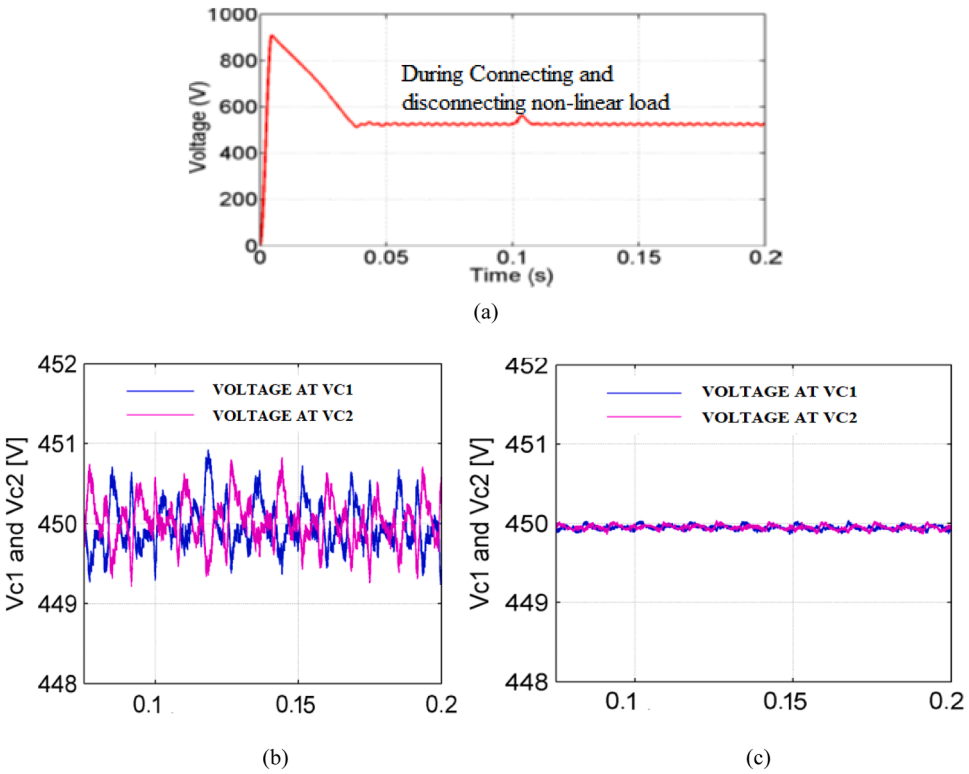

Fig. 16. (a) DC-link voltage waveform (b) Capacitor Voltage at VC1 and VC2 before compensation (c) Capacitor Voltage at VC1 and VC2 after compensation.

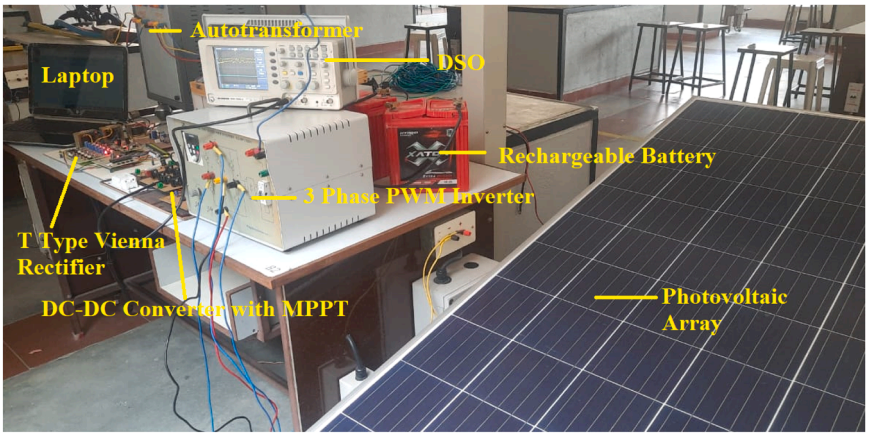

Fig. 17. Experimental setup.

for fast EV battery charging stations with IIPQ control strategy has been tested initially with the help of Simulink MATLAB. The main design parameters considered for simulation and prototype model is mentioned in Table 5 along with respective ranges.

To examine and validate these system, MATLAB Simulink results has been dually verified along with laboratory prototype results for three different cases as i) input supply with balanced load, ii) balanced input supply with non-linear load and iii) unbalanced input supply with non-linear load condition.

Case (i): Balanced input supply with balanced/static load

The system is validated under balanced state of both input supply and load condition. EV charging station rectifier unit consists of RL network with diode switch or T-Type Vienna rectifier circuit act as non-linear load and RL circuit act as linear load. Load side distorted 3 phase current waveform before compensation and injected current after compensation are shown in Fig. 9(a) and 9(b) respectively. Then the effectiveness of the compensation system after integrates with this system provides smooth source current which is shown in Fig. 9(c).

Fig. 10 shows the THD analysis of before and after connecting this control strategy for A phase. THD value obtained before compensation as 21.77% and value obtained after compensation with this proposed system as 2.95% which is permissible limit as per IEEE standard.

Fig. 11(a) and 11(b) shows the solar PV array voltage generated with PV array and stable voltage maintained at DC link capacitor voltage respectively during both connecting and disconnecting Vienna rectifier for EV fast charging purpose.

Case (ii): Balanced input supply with non-linear (dynamic) load condition

The proposed system is validated under balanced state of input supply and dynamic load condition. Load side distorted 3 phase waveforms before compensation and also injected current after compensation are shown in Fig. 12(a) and 12(b) respectively. Fig. 12 (c) and 12 (d)

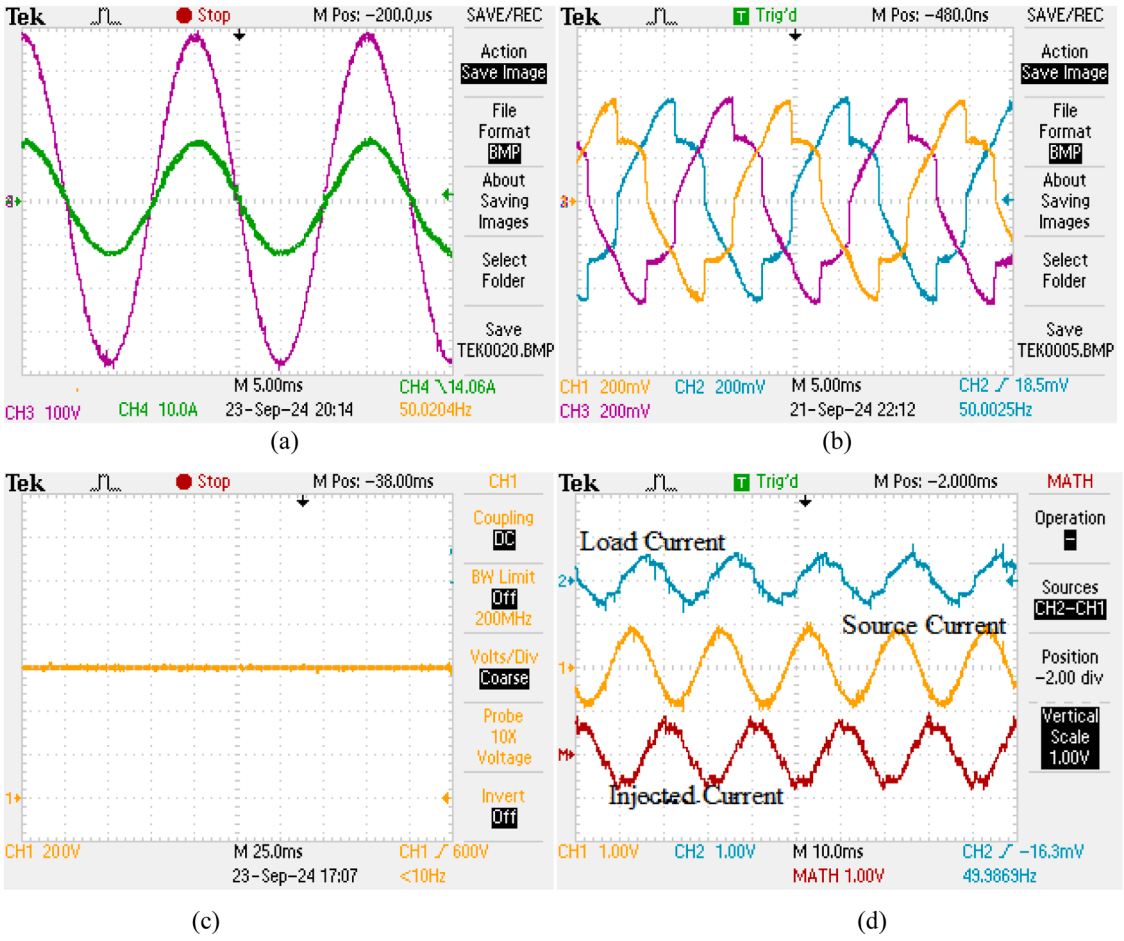

Fig. 18. (a) Load side current and voltage during static condition (b) Distorted load side three phase current (c) Constant DC link voltage (d) Current waveforms during compensation.

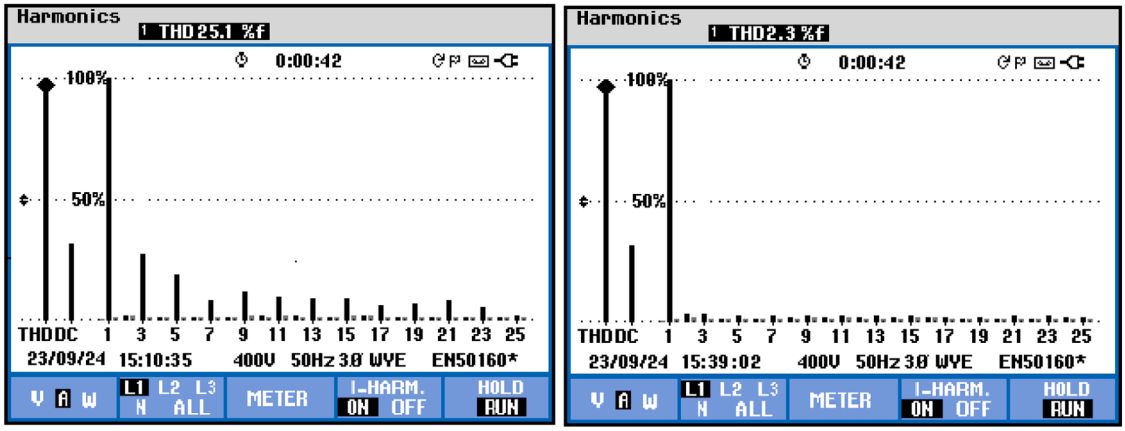

Fig. 19. A-Phase THD Spectrum analysis for before and after connecting IIPQ control.

shows the Source Current after Compensation and Compensated Reactive Power which shows the effectiveness and better efficiency of the proposed system.

Fig. 13 shows the spectral analysis of THD for before and after connecting this control strategy for B phase in this balanced input side supply with dynamic (non-linear) load condition. THD value obtained before compensation as 23.15% and value obtained after compensation with this proposed system as 2.93% which is permissible limit as per IEEE standard.

Case (iii): Unbalanced input Supply with non-linear (dynamic load) condition

The proposed system efficiency and adaptability is examined with unbalanced input supply with non-linear (dynamic) load condition. Fig. 14 (a) and Fig. 14 (b) depicts the distorted 3 phase load current waveform and injected current for compensation respectively. Fig. 14 (c) and Fig. 14 (d) depicts the 3-phase source current after compensation and 3 phase unbalanced supply voltage respectively.

Fig. 15 shows the spectral analysis of THD for before and after

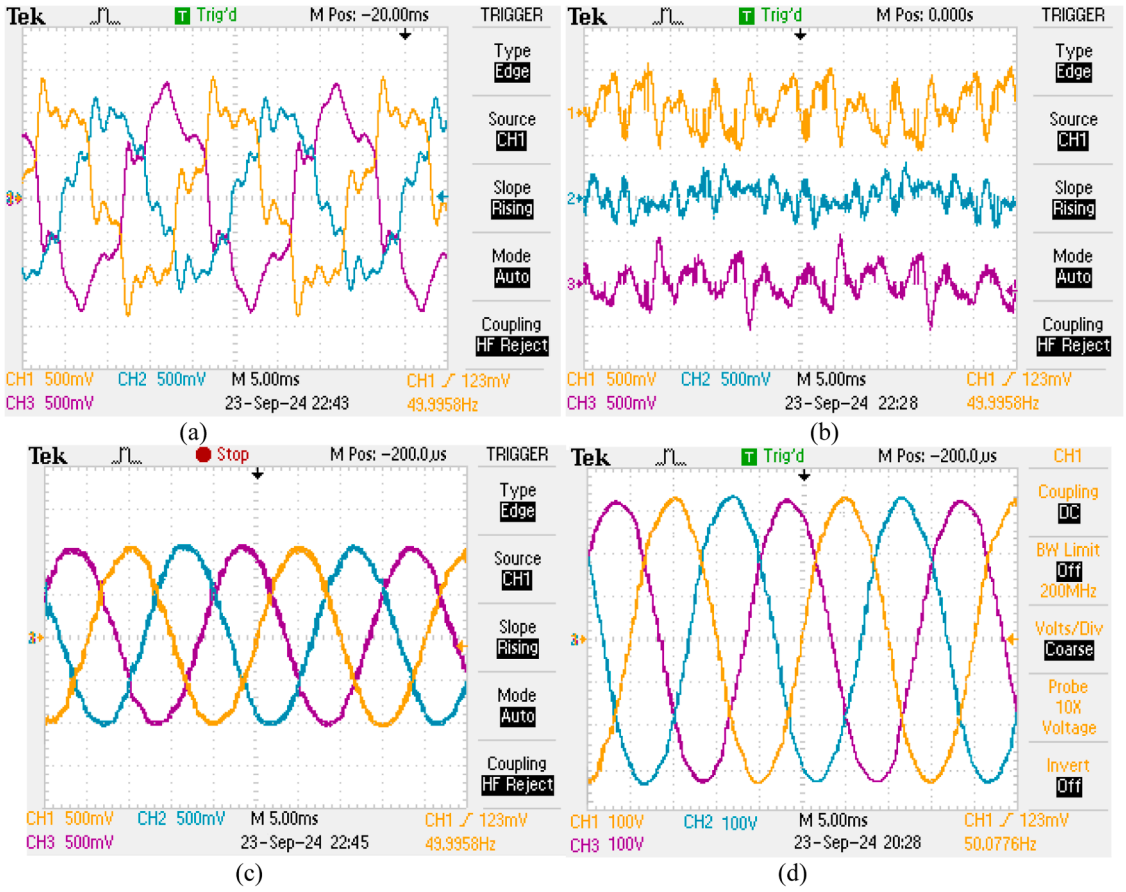

Fig. 20. (a) Distorted load side current before connecting the compensation unit (b) Injecting compensate current at source side (c) Compensated source current (d) Balanced source side voltage.

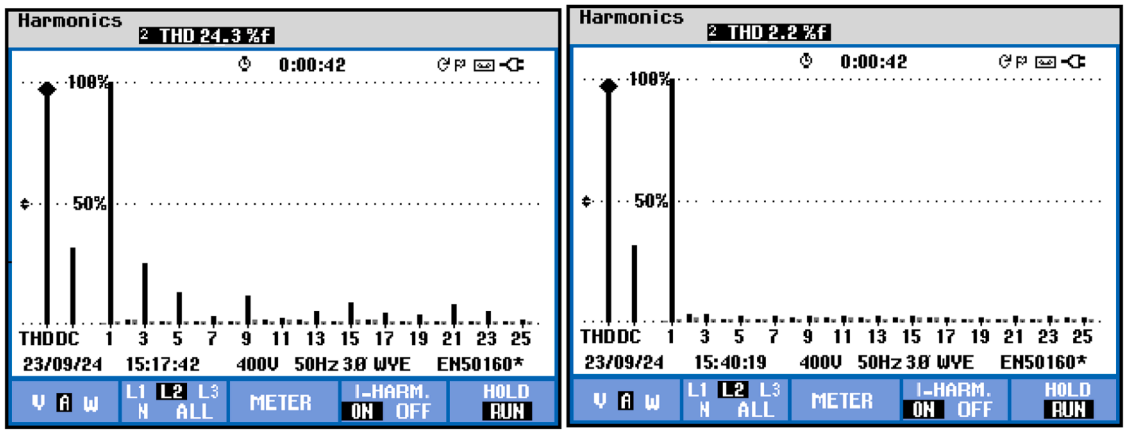

Fig. 21. B- Phase spectral analysis of THD for before and after compensation.

interface this control strategy for C phase in this unbalanced input supply with non-linear load condition. THD value obtained before compensation as 22.17% and value obtained after compensation with this proposed system as 2.32% which is permissible limit as per IEEE standard. Fig. 16 shows the stability of DC-Link voltage with minimal distortion during connecting and sudden disconnection of non-linear load with this system i.e during fast EV charging.

Fig. 16 (a) depicts the DC-Link Voltage during connecting and disconnecting of non-linear load during EV charging. Fig. 16 (b) depicts the rectifier Capacitor Voltage at VC1 and VC2 before compensation Fig. 16 (c) depicts the rectifier Capacitor Voltage at VC1 and VC2 after compensation which is balanced by proportional integral control. Finally, as per this MATLAB Simulink result analysis of the proposed FLC- based IIPQ control stratergy plays effective role to reduce the harmonics level and also stabilize the current distortion during connecting and disconnecting of rectifier unit in OFF board EV charging stations.

Prototype validation of FLC tuned PI – IIPQ control-based shunt APF

To validate the feasibility and efficiency of the proposed control

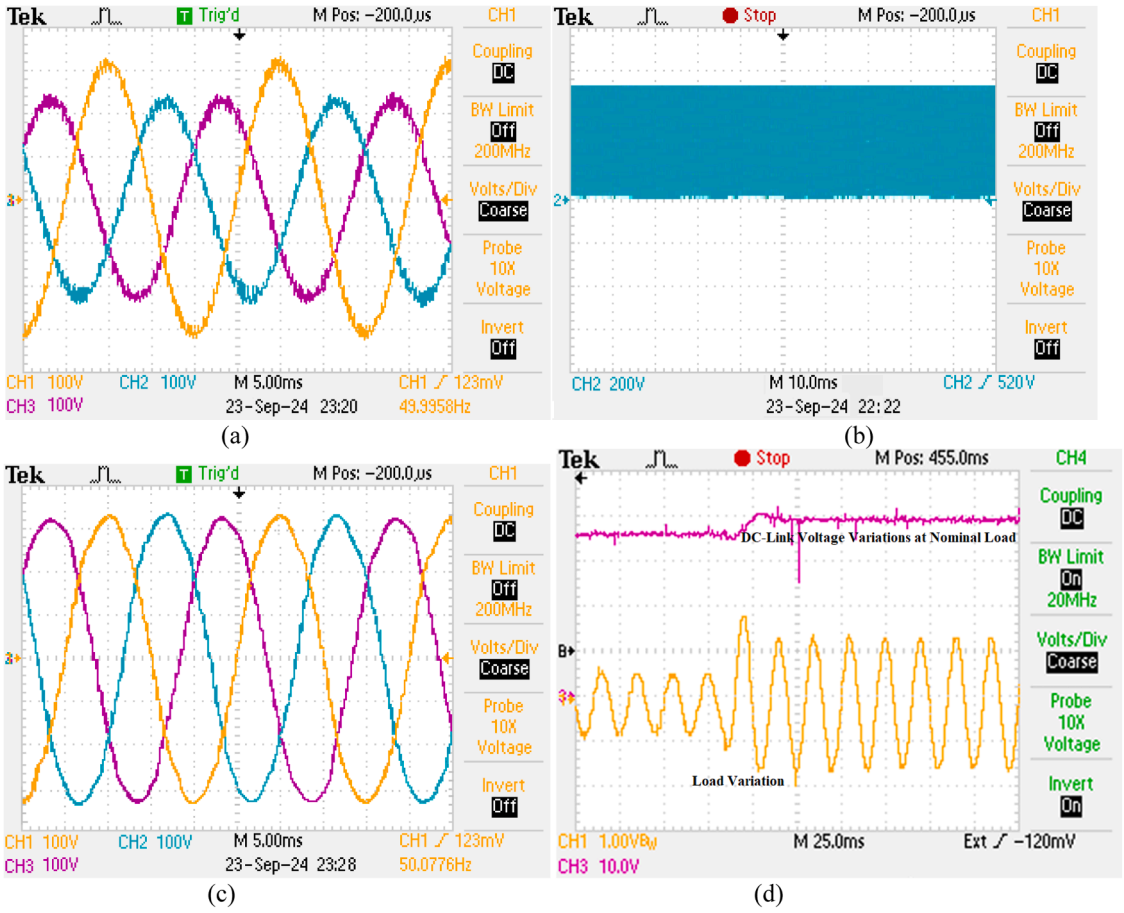

Fig. 22. shows (a) distorted unbalanced source side voltage (b) DC-Link voltage at DC side capacitor (c) compensated load side voltage after compensation (d) Distorted load side current before compensation.

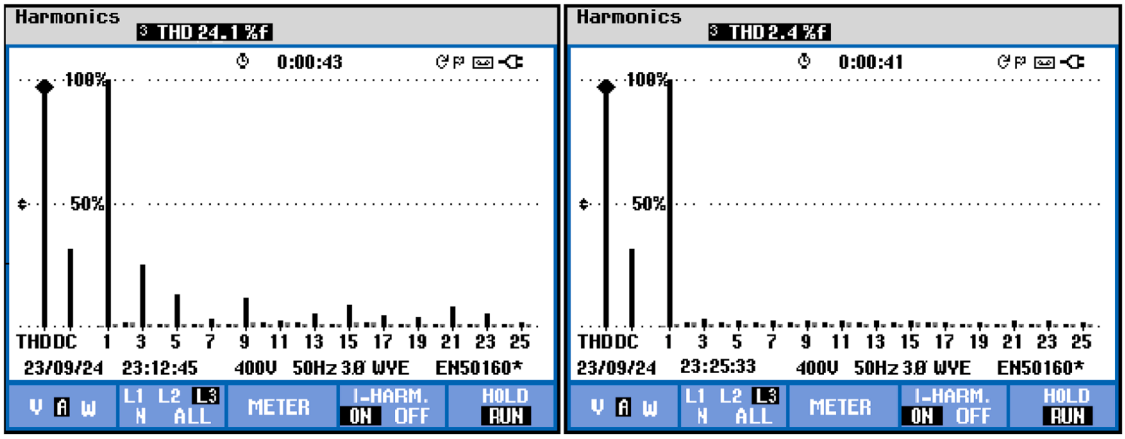

Fig. 23. C- Phase Spectral analysis of THD for before and after compensation.

strategy in OFF board fast EV charging station was tested with 320V prototype experimental setup. The entire experimental setup includes a SPV array with battery charging unit, a DC-DC converter with PWM controller, a voltage source inverter with SAPF, a unidirectional PI-FLC based TTVR and battery storage unit. The entire voltage and current parameters get tuned by using dsPIC30F4011 controller interfaced with the grid system. Fig. 17 shows the working prototype model with IIPQ control strategy. Both simulation and hardware tests are done with similar values which was given in Table 3. The obtained results implies that the adoptability and feasibility is more for DC fast charging stations.

Hardware results and discussion

In this research, prototype model was developed and tested under the following three different test cases as Balanced input supply with linear load condition, Balanced input supply with non-linear load condition and Unbalanced input Supply with non-linear Load Condition. All the test cases have been verified to check the implementation feasibility as well as THD suppression through FLC tuned PI controller based IIPQ control technique. Following Fig. 18 represents the results obtained under the balanced input supply with linear load test case. Fig. 18 (a)

Table 6
Comparative THD spectral analysis of three cases in simulation and experimental setup.

Simulation Study						
Phases	THD% Obtained before connecting compensation- Load Side at EV Charging station			THD% Obtained after connecting FLC-IIPQ control with TTVR - Load Side at EV Charging station		
	Case-1	Case-2	Case-3	Case-1	Case-2	Case-3
A	21.77	22.51	21.48	2.95	2.62	2.13
B	22.98	23.15	22.13	2.98	2.93	2.13
C	22.56	23.54	22.17	2.46	2.42	2.32
Experimental Study						
A	25.1	24.61	24.84	2.3	2.1	2.4
B	25.2	24.3	24.6	2.1	2.2	2.6
C	24.7	23.9	24.1	2.4	2.5	2.4

shows the Load side current and voltage during stable condition Fig. 18 (b) shows the distorted load side three phase current. Fig. 18(c) shows the constant DC link voltage at the DC side. Fig. (d) shows the Load, source and injected current measured during compensation.

Fig. 19 shows the spectral analysis of THD for both before and after compensation. As a result, measured in A-phase as 25.1 % before compensation and the harmonic level get reduced to 2.3% after compensation which shows that the system is suitable to mitigate the harmonic as per the IEEE standard limit.

During balanced input supply with non-linear load condition case, Fig. 20 (a) shows the distorted load side three phase current before connecting the compensation unit. Fig. 20 (b) shows the injecting compensate current at source side to stabilize the grid system. Fig. 20 (c) and Fig. 20 (d) shows the compensated source current after compensation and balanced source side voltage respectively.

Fig. 21 shows the spectral analysis of THD with proposed system. As a result, measured in B-phase as 24.3 % before compensation and the harmonic level get reduced to 2.2% once connecting the compensation system. Fig. 22 (a) depicts the distorted unbalanced source side voltage while connecting unbalanced loads in network. Fig. 22 (a) depicts the DC-Link voltage level at DC side capacitor. Fig. 22 (c) shows compensated load side voltage after interface the IIPQ control strategy. Fig. 22 (d) describes that Distorted load side current before compensation

Fig. 23 shows the spectral analysis of THD with proposed system. As a result, measured in C-phase as 24.1 % before compensation and the harmonic level get reduced to 2.4% after compensation.

As per this developed prototype results obtained under all three test cases, this methodology is highly suitable for high power fast charging applications without any voltage and current harmonic disturbances. Moreover, DC link voltage has maintained as 520 V always with the support of SPV generating unit integrated with FLC based IIPQ control strategy. SPV system operates in three different modes to achieve the constant DC-link voltage along with battery storage unit. Here the smooth voltage gain without any voltage stress has been obtained with IRFP260-Mosfet switches and appropriate filter inductor used in DC-DC power conversion based on continuous conduction. Here, the DC-Link capacitor value design calculations are discussed with suitable mathematical expression. FLC tuned PI controller have been interfaced with this topology to improvise the system performance under dynamic load changing conditions, ensure the precise control of voltage balance at the

Table 7
Performance comparison of various charging converters used in EV.

Reference	Various Charging Converters	Controller Type used	Power Range Used (Kw)	No. of Switches used with diode	Mitigating Power Quality issues addressed	General Operating Service	THD %	Advantages and Applications
[27]	Unidirectional DC-DC Boost Converter	Drive Frequency Converter	250	12	No	G2V	>30	▪ Fast battery charging ▪ Used in DC Micro grid
[28]	Matrix converter	Ultra-high voltage AC/DC isolated matrix	300	12	No	V2G	>22	▪ Optimized modulation strategy ▪ Bidirectional power flow
[29]	Swiss Converter	Current-compensated integrated common-mode coupled inductor	8	12	No	DC Distributed System	No	▪ Bidirectional power flow ▪ Used in Aircraft and EV Charger
[30]	Minnesota Converter	Direct Torque Control	15	12	yes	G2V	>8	▪ Used in EV Charger
[31]	Vienna Rectifier for Level 1 charging	SVM Control	1.5	21	Yes	General applications	No	▪ Rapid charging ▪ Greater power factor adjustment ▪ On Board
[32]	Vienna Rectifier for Level 2 charging	Mixed-signal based control	12	18	yes	G2V, V2G	4.7	▪ Rapid charging ▪ EV as well as Welding power supplies ▪ On Board
[33]	Two-stage inductive-power-transfer (TSIPT) to pology	Constant Power (CP) control strategy	15.3	18	No	Wireless Power Transfer charger	No	▪ Fast Charging ▪ Wireless ▪ EMI issues ▪ Constant charging output
[34]	Bidirectional DC-DC Buck- boost converter	Zero Voltage Turn-on (ZVT) strategy	5	18	No	G2V	No	▪ DC link Voltage stability ▪ Off Board
Proposed Work	**Vienna Rectifier for Level 3 charging**	**IIPQ Control strategy**	**30**	**18**	**Yes**	**G2V**	**2.5**	▪ **Fast EV Charging** ▪ **Suppressed Harmonic issues** ▪ **Better stability** ▪ **OFF Board**

capacitor C1 and C2 in TTVR as well as DC-link voltage with reduced harmonic distortions. Furthermore, the proposed IIPQ control strategy is utilized to generate reference signal to actuate the switches through Hysteresis Current Control (HCC) technique. Table 6 shows the comparative study of THD% obtained from simulation and experimental setup irrespective of all the three phases with mentioned three test cases. In all the cases, the THD value obtained is below 5% as per IEEE 519 standard. Table 7 shows the performance comparisons of various converter along with Vienna rectifier while used in EV charging applications. Based on the literature, Vienna rectifier is superior in terms of size, speed of operation, THD level, power factor improvement and efficiency.

Conclusion

In this paper, a FLC based IIPQ control approach has been presented for T-Type Vienna Rectifier along with balanced capacitor voltage at fast EV charging station. The proposed IIPQ research strategy is employed with adoptive instantaneous current signal extraction with transform three phase *abc* coordinates to $\alpha\beta$ coordinated by Clarke's transformation. Moreover, the proposed system provides superiority solution to minimize the current harmonics and also reactive compensation in OFF board fast EV charging station. This system readily supports for both steady state load conditions as well as unbalanced load variations with constant DC-Link voltage at Capacitors VC1 and VC2. SPV unit interfaced with shunt active filter provides stable support to utility grid at PCC if any discontinuity occurs in distribution network. The Inc conductance MPPT technique is used to improve the efficiency of the SPV generation and battery storage unit has been used to compensate the supply needs during unfavorable working state of PV array and distribution grid. Additionally, this SPV based system charging stations helps to environment by reducing CO2 emissions and other toxic gases. The proposed optimization technique has been examined and checked the practical feasibility with the help of MATLAB Simulink and prototype model with 15 KW. The validation shows the comparative analysis of both simulation and hardware results, identifies THD% value obtained in all three phases as up to 2.5% only which is lesser than ceiling limit of IEEE 519 standard. Hence, this method is more suitable for the OFF-board EV charging and high-power applications. The main limitations are due to high switching frequency, non-isolated converter and fast charging current leads to induce significant thermal stress on rectifier switches which require suitable heat sink and safety precautions. Furthermore, this research only looked solar based energy to maintain DC-Link and capacitor voltage balance, in addition to this system add wind energy can make more stability and overcoming the restrictions.

Following Abbreviations are used in this manuscript

EV	Electric Vehicle
G2V	Grid-to-Vehicle
DC	Direct Current
dsPIC	Digital signal Peripheral Interface Controller
TTVR	T-Type Vienna Rectifier
THD	Total Harmonic Distortion
MPPT	Maximum Power Point Tracking
MOSFET	Metal Oxide Semiconductor Field Effect Transistor
SPV	Solar Photovoltaic
SAF	Shunt Active Filter
PCC	Point of Common Coupling
PWM	Pulse Width Modulation
PI	Proportional Integral
FLC	Fuzzy Logic Controller
IIPQ	Improved Instantaneous real and reactive power
IEEE	Institute of Electrical and Electronics Engineers
PQ	Power Quality

CRediT authorship contribution statement

Suresh Kalichikadu Paramasivam: Writing – original draft, Software, Methodology, Investigation, Conceptualization. **Ramesh Senniyappan:** Writing – review & editing, Supervision, Investigation. **Senthil Kumar Ramu:** Validation, Investigation, Formal analysis. **Senthilkumar Mani:** Writing – review & editing, Visualization, Validation.

Declaration of competing interest

The authors declare that they have no known competing financial interests or personal relationships that could have appeared to influence the work reported in this paper.

Data availability

Data will be made available on request.

References

[1] M.R. Khalid, I.A. Khan, S. Hameed, M.S. Asghar, J. Ro, A comprehensive review on structural topologies, power levels, energy storage systems, and standards for electric vehicle charging stations and their impacts on Grid, IEEe Access. 9 (2021) 128069–128094, https://doi.org/10.1109/access.2021.3112189.

[2] E. Giannakis, D. Serghides, S. Dimitriou, G. Zittis, Land Transport Co2 Emissions and Climate Change: Evidence from cyprus, Int. J. Sustain. Energy 39 (7) (2020) 634–647, https://doi.org/10.1080/14786451.2020.1743704.

[3] C.A.Vaithilingam G.Rajendran, N. Misron, K. Naidu, M.R. Ahmed, A comprehensive review on System Architecture and international standards for Electric Vehicle Charging stations, J. Energy Storage 42 (2021) 103099, https://doi.org/10.1016/j.est.2021.103099.

[4] J. Yuan, L. Dorn-Gomba, A.D. Callegaro, J. Reimers, A. Emadi, A review of bidirectional on-board chargers for Electric Vehicles, IEEe Access. 9 (2021) 51501–51518, https://doi.org/10.1109/access.2021.3069448.

[5] A.U. Rehman, M.F. Zia, Harism. Khalid, Z. Said, S.M. Muyeen, Wind and grid energy-based onshore beach charging station for electric vehicles: An integration infrastructure with techno economics, Sustainable Mobility, and environmental protection, Results. Eng. 26 (2025) 105113, https://doi.org/10.1016/j.rineng.2025.105113.

[6] B.H. Jiang, C.-C. Hsu, N.-W. Su, C.-C. Lin, A review of Modern Electric Vehicle Innovations for Energy Transition, Energies. (Basel) 17 (12) (2024) 2906, https://doi.org/10.3390/en17122906.

[7] N. Vijaya Anand, Y. Naveen, Small-signal modelling of Bidirectional CLLC converters for onboard charging application in electric vehicles, Int. J. Circuit Theory Appl. (Jan. 2025), https://doi.org/10.1002/cta.4431.

[8] W. Khan, F. Ahmad, M.S. Alam, Fast EV charging station integration with grid ensuring optimal and Quality Power Exchange, Eng. Sci. Technol., Int. J. 22 (1) (2019) 143–152, https://doi.org/10.1016/j.jestch.2018.08.005.

[9] A. Darvish Falehi, E. Salary, An innovative high-gain multi-stage non-isolated step-up converter controlled by optimal interval type-2 fuzzy system based maximum power point tracking, Results. Eng. 24 (2024) 103458, https://doi.org/10.1016/j.rineng.2024.103458.

[10] A. Balal, M. Giesselmann, Design of a level-3 electric vehicle charging station using a 1-MW solar system via the Distributed Maximum Power Point Tracking Technique, Clean Energy 8 (1) (2024) 23–35, https://doi.org/10.1093/ce/zkad084.

[11] H.S. Das, M.M. Rahman, S. Li, C.W. Tan, Electric vehicles standards, charging infrastructure, and impact on grid integration: A Technological Review, Renew. Sustain. Energy Rev. 120 (2020) 109618, https://doi.org/10.1016/j.rser.2019.109618.

[12] B. Palaniyappan, K.R S, T. V, Dynamic pricing for load shifting: Reducing Electric vehicle charging impacts on the grid through machine learning-based demand response, Sustain. Cities. Soc. 103 (Apr. 2024) 105256, https://doi.org/10.1016/j.scs.2024.105256.

[13] A.U. Rehman, et al., Techno Economics and Energy Dynamics of a solar powered smart charging infrastructure for electric vehicles with advanced IOT based monitoring and RFID based security, Sustainable Futures 8 (2024) 100376, https://doi.org/10.1016/j.sftr.2024.100376.

[14] S. Kalichikadu Paramasivam, S.K. Ramu, P. Cholamuthu, Unit vector template control strategy-based harmonic mitigation and charging with three phase–three level–three switch Vienna rectifier for Level 3 Electric Vehicle Charging Applications, Int. J. Circuit Theory Appl. 52 (6) (Dec. 2023) 2889–2915, https://doi.org/10.1002/cta.3904.

[15] J. Lei, et al., An improved three-phase buck rectifier topology with reduced voltage stress on transistors, IEEe Trans. Power. Electron. 35 (3) (2020) 2458–2466, https://doi.org/10.1109/tpel.2019.2931803.

[16] G. Rajendran, C.A. Vaithilingam, N. Misron, K. Naidu, M.R. Ahmed, Voltage Oriented Controller based Vienna Rectifier for Electric Vehicle Charging stations,

IEEe Access. 9 (2021) 50798–50809, https://doi.org/10.1109/access.2021.3068653.
[17] L. Ta, N. Dao, D.-C. Lee, High-efficiency hybrid LLC resonant converter for on-board chargers of plug-in electric vehicles, IEEe Trans. Power. Electron. 35 (8) (2020) 8324–8334, https://doi.org/10.1109/tpel.2020.2968084.
[18] V. Monteiro, J.C. Ferreira, A.A. Nogueiras Melendez, C. Couto, J.L. Afonso, Experimental validation of a novel architecture based on a dual-stage converter for off-board fast battery chargers of electric vehicles, IEEe Trans. Veh. Technol. 67 (2) (2018) 1000–1011, https://doi.org/10.1109/tvt.2017.2755545.
[19] K. Sun, X. Lin, Y. Li, Y. Gao, L. Zhang, Improved modulation mechanism of parallel-operated T-type three-level PWM rectifiers for neutral-point potential balancing and circulating current suppression, IEEe Trans. Power. Electron. 33 (9) (2018) 7466–7479, https://doi.org/10.1109/tpel.2017.2772025.
[20] A.U. Rehman, H.M. Khalid, S.M. Muyeen, Grid-integrated solutions for sustainable EV charging: A Comparative Study of renewable energy and Battery Storage Systems, Front. Energy Res. 12 (Sep. 2024), https://doi.org/10.3389/fenrg.2024.1403883.
[21] J. Wang, S. Ji, S. Liu, H. Jiang, W. Jiang, A discontinuous PWM strategy to control neutral point voltage for Vienna rectifier with improved PWM sequence, IEEe J. Emerg. Sel. Top. Power. Electron. 10 (3) (2022) 3230–3241, https://doi.org/10.1109/jestpe.2021.3120540.
[22] Z. Hou, D. Jiao, B.C. Gutierrez, J.-S. Lai, P.-L. Chen, Design of a 15kw high-efficiency and high power density bidirectional TCM Buck/Boost Converter, 2024 IEEE Appl. Power Electron. Conf. Exposition (APEC) (2024) 341–347, https://doi.org/10.1109/apec48139.2024.10509033.
[23] D. Chou, K. Fernandez, R.C. Pilawa-Podgurski, An interleaved 6-level gain bidirectional converter for Level II Electric Vehicle charging, 2019 IEEE Appl. Power Electron. Conf. Exposition (APEC) (2019) 594–600, https://doi.org/10.1109/apec.2019.8721971.
[24] R.K. Lenka, A.K. Panda, A.R. Dash, N.N. Venkataramana, N. Tiwary, Reactive power compensation using vehicle-to-grid enabled bidirectional off-board EV Battery Charger, in: 2021 1st International Conference on Power Electronics and Energy (ICPEE), 2021, pp. 1–6, https://doi.org/10.1109/icpee50452.2021.9358582.
[25] B. Zhang, S. Xie, X. Wang, J. Xu, Modulation method and control strategy for full-bridge-based Swiss rectifier to achieve ZVS operation and suppress low-order harmonics of injected current, IEEe Trans. Power. Electron. 35 (6) (2020) 6512–6522, https://doi.org/10.1109/tpel.2019.2951795.
[26] B. Bharaneedharan, P. Suresh, P.V. Elumalai, Energy-efficient Vienna rectifier for electric vehicle battery charging stations, Results. Eng. 23 (2024) 102671, https://doi.org/10.1016/j.rineng.2024.102671.
[27] B. Singh, et al., A review of three-phase improved power quality AC–DC converters, IEEE Trans. Ind. Electron. 51 (3) (Jun. 2004) 641–660, https://doi.org/10.1109/tie.2004.825341.
[28] M.A. Waghmare, B.S. Umre, M.V. Aware, A. Kumar, S.A. Yerkal, Common-mode voltage minimization in three-phase to six-phase indirect matrix converter using virtual vector synthesization, IEEe Trans. Ind. Appl. 58 (4) (Jul. 2022) 4848–4858, https://doi.org/10.1109/tia.2022.3166456.
[29] T. Langbauer, et al., Third-harmonic-type modulation minimizing the DC-link energy storage requirement of isolated phase-modular three-phase PFC rectifier systems, IEEe Access. 11 (2023) 34359–34371, https://doi.org/10.1109/access.2023.3261243.
[30] D. Menzi, et al., Novel bidirectional single-stage isolated three-phase Buck-Boost PFC rectifier system, 2023 IEEE Appl. Power Electron. Conf. Exposition (APEC) (Mar. 2023) 1936–1944, https://doi.org/10.1109/apec43580.2023.10131553.
[31] J. Zou, C. Wang, H. Cheng, J. Liu, Triple line-voltage cascaded Vienna converter applied as the medium-voltage AC Drive, Energies. (Basel) 11 (5) (Apr. 2018) 1079, https://doi.org/10.3390/en11051079.
[32] Y.-D. Kwon, J.-H. Park, K.-B. Lee, Improving line current distortion in single-phase Vienna rectifiers using model-based predictive control, Energies. (Basel) 11 (5) (May 2018) 1237, https://doi.org/10.3390/en11051237.
[33] O. Seghyar, et al., A 15 KW level 3 inductive power transfer charger for fast charging and maximum efficiency, Results. Eng. 24 (Dec. 2024) 102868, https://doi.org/10.1016/j.rineng.2024.102868.
[34] W. Christopher I, et al., A bidirectional DC/DC converter for renewable energy source-fed EV charging stations with enhanced DC link voltage and Ripple Frequency Management, Results. Eng. 24 (Dec. 2024) 103469, https://doi.org/10.1016/j.rineng.2024.103469.